Supplementary Figures and Legends

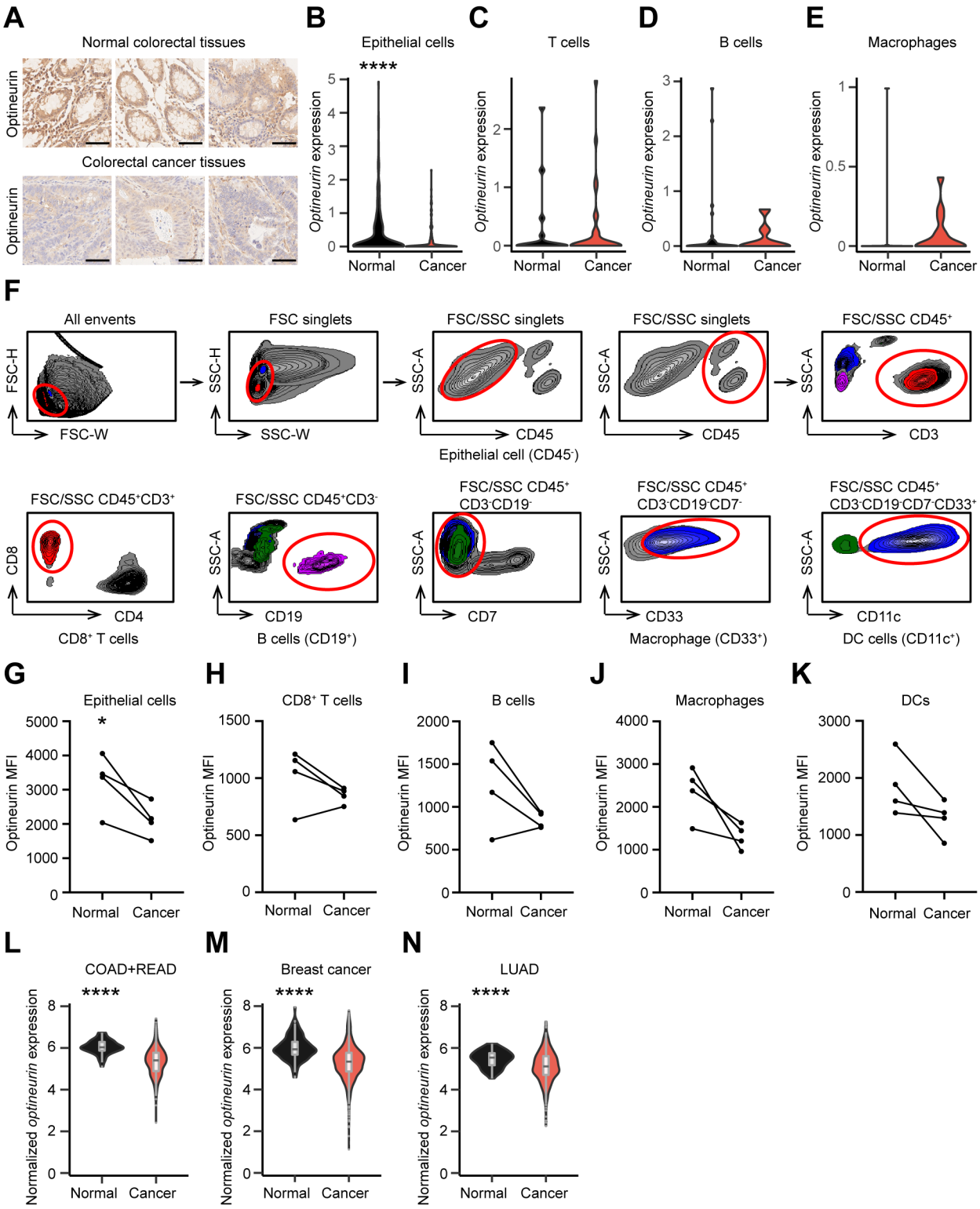

Supplementary Figure S1. Optineurin expression in normal and cancer tissues

A, Optineurin protein expression in colorectal cancer tissues and paired adjacent normal colorectal tissues. Representative immunohistochemistry staining images showed optineurin expression. (cohort 1) (n = 66). Scale bars, 50 μm.

B - E, Single cell analysis of *optineurin* transcripts in colorectal cancer tissues and adjacent normal colorectal tissues. *Optineurin* expression was determined in (**B**) epithelial cells, (**C**) T cells ($P = 0.95$), (**D**) B cells ($P = 0.95$), and (**E**) macrophages ($P = 0.15$). n = 11. Two tailed t-tests, ****$P < 0.0001$

F - K, Optineurin protein expression in colorectal cancer tissues and adjacent normal colorectal tissues. (**F**)**,** Flow cytometry gating strategy determining different cell subsets in the human colorectal tissues. Optineurin protein expression was determined by flow cytometry analysis in (**G**) epithelial cells, (**H**) $CD8^+$ T cells ($P = 0.1925$), (**I**) B cells ($P = 0.135$), (**J**) macrophages ($P = 0.0605$), and (**K**) dendritic cells (DCs) ($P = 0.1029$). n = 4. Paired t-tests, *$P < 0.05$.

L - N, *Optineurin* transcripts in different normal tissues and cancer tissues. *Optineurin* transcripts were quantified in (**L**) normal colorectal tissues (n = 51), colorectal cancer (COAD+ READ) tissues (n = 380), (**M**) normal breast tissues (n = 113), breast cancer tissues (n = 1098), (**N**) normal lung tissues (n = 59), and lung cancer (LUAD) tissues (n = 515) in TCGA data set. Two tailed t-tests, ****$P < 0.0001$

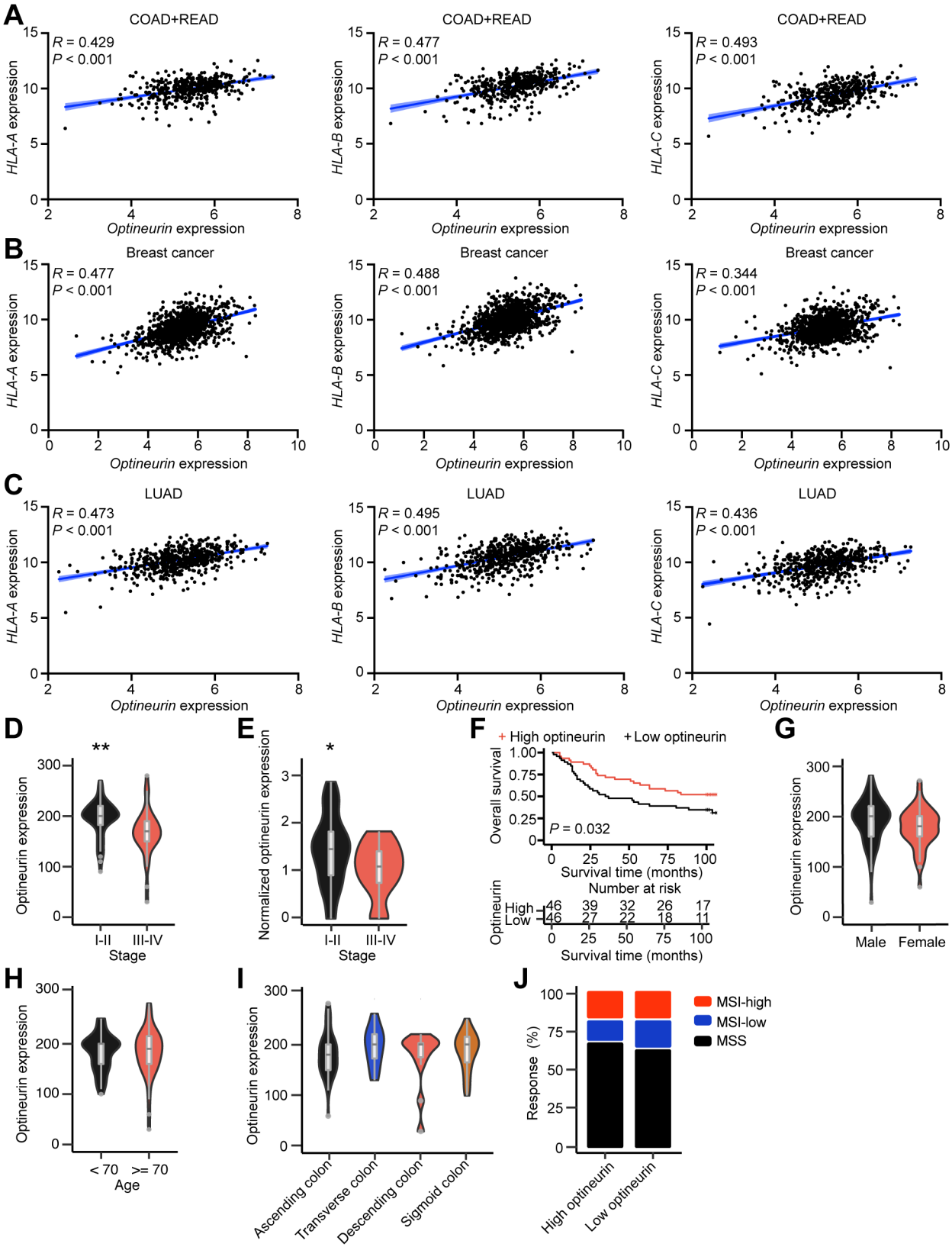

Supplementary Figure S2. Tumor optineurin correlates with patients' immune and clinicopathological features

A - C, Correlation analysis of optineurin and MHC-I (HLA-A, HLA-B, and HLA-C) expression in different cancers. Correlation of *optineurin* expression with *HLA-A*, *HLA-B*, and *HLA-C* in (**A**) colorectal cancer (COAD+READ) tissues (n = 431), (**B**) breast cancer tissues (n = 1211), and (**C**) lung cancer (LUAD) tissues (n = 574) in TCGA data set.

D and **E,** Optineurin expression in different TNM stages in colorectal cancer tissues. (**D**), Optineurin expression detected by immunohistochemistry staining in different TNM stages of colorectal cancer (n = 92). Two tailed t-tests, $^{**}P < 0.01$. (**E**), Proteomic analysis of optineurin expression in different TNM stages of colorectal cancer (n = 90). Two tailed t-tests, $^{*}P < 0.05$.

F, Survival comparison between patients with low (n = 46) and high (n = 46) levels of optineurin in patients with colorectal cancer in cohort 1 (n = 92), Log-rank test.

G - I, Correlation of optineurin expression with patient gender (**G**) ($P = 0.1577$), age (**H**) ($P = 0.8262$) (Two tailed t-tests), and tumor location (**I**) ($P = 0.3486$) (Spearman's rank correlation).

J, Relationship between optineurin protein expression and MSI status. The MSI status is shown in colon cancer patients with high and low optineurin expression (median). Chi-square test, $P = 0.863$.

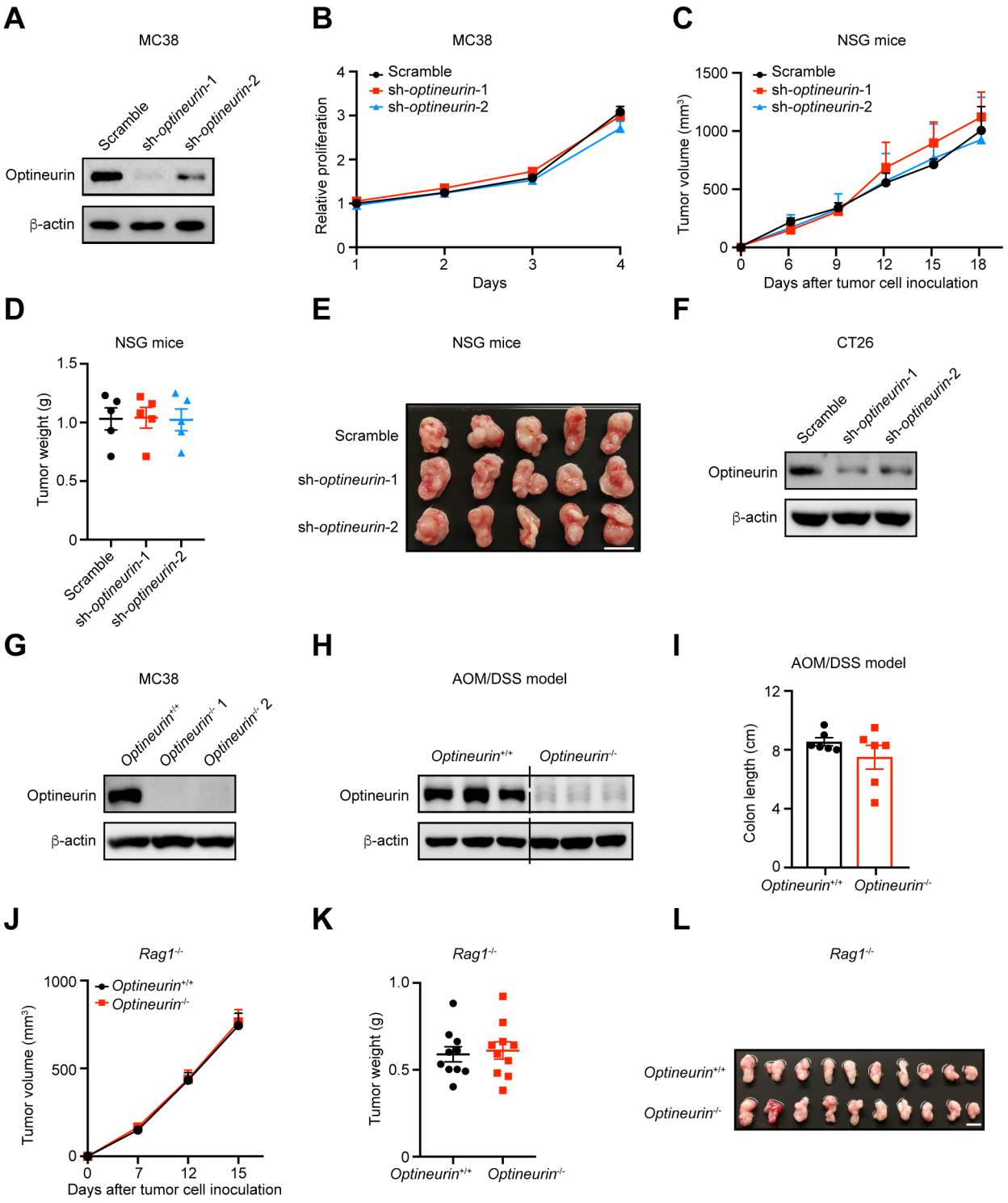

Supplementary Figure S3. Effect of optineurin deficiency on tumor growth

A, Efficacy of sh-*optineurin* on tumor optineurin expression. Immunoblots analysis revealed optineurin expression in sh-*optineurin* (sh-*optineurin*-1 and sh-*optineurin*-2) and scrambled shRNA expressing MC38 tumor cells. One of 3 repeats is shown.

B, Effect of optineurin expression on MC38 cell proliferation. sh-*optineurin* and scrambled shRNA expressing MC38 cell proliferation was detected with Alamar Blue reagents. Values are means ± SD. n = 3 independent experiments. Two-way ANOVA, scrambled shRNA vs. sh-*optineurin*-1, $P > 0.05$; scrambled shRNA vs. sh-*optineurin*-2, $P > 0.05$.

C - E, Effect of optineurin expression on MC38 tumor growth in NSG mice. sh-*optineurin* and scrambled shRNA expressing MC38 tumor cells were inoculated into NSG mice. Tumor volume (**C**), tumor weight (**D**), and tumor images (**E**) are shown. Mean ± SEM, n = 5 /group. Two-way ANOVA, scrambled shRNA vs. sh-*optineurin*-1, $P > 0.05$; scrambled shRNA vs. sh-*optineurin*-2, $P > 0.05$ (**C**). Two tailed t test, shRNA vs. sh-*optineurin*-1, $P > 0.05$; scrambled shRNA vs. sh-*optineurin*-2, $P > 0.05$ (**D**). Scale bars, 1 cm (**E**).

F, Efficacy of sh-*optineurin* on tumor optineurin expression. Immunoblots showed optineurin expression in sh-*optineurin* (sh-*optineurin*-1 and sh-*optineurin*-2) and scrambled shRNA expressing CT26 tumor cells. One of 3 repeats is shown.

G, Efficacy of optineurin knock out on tumor optineurin expression. Immunoblots showed optineurin expression in 2 *optineurin*$^{-/-}$ MC38 clones and *optineurin*$^{+/+}$ (wild type) MC38 tumor cells. One of 3 repeats is shown.

H and **I**, Effect of IEC-optineurin knock-out on colorectal tumorigenesis in AOM/DSS model. (**H**) Immunoblots showed optineurin expression in IEC of *optineurin*$^{+/+}$ or *optineurin*$^{-/-}$ mice. 3 mice /group. (**I**) Colorectal length of *optineurin*$^{+/+}$ or *optineurin*$^{-/-}$ mice is shown. 6 mice /group. Two tailed t test, $P > 0.05$.

J - L, Effect of optineurin expression on MC38 tumor growth in *Rag1*$^{-/-}$ mice. *Optineurin*$^{-/-}$ and *optineurin*$^{+/+}$ MC38 tumor cells were inoculated into *Rag1*$^{-/-}$ mice. Tumor volume (**J**), tumor weight (**K**), and tumor images (**L**) are shown. Two-way ANOVA, *optineurin*$^{+/+}$ vs *optineurin*$^{-/-}$, $P > 0.05$ (**J**). Two tailed t test, $P > 0.05$ (**K**).

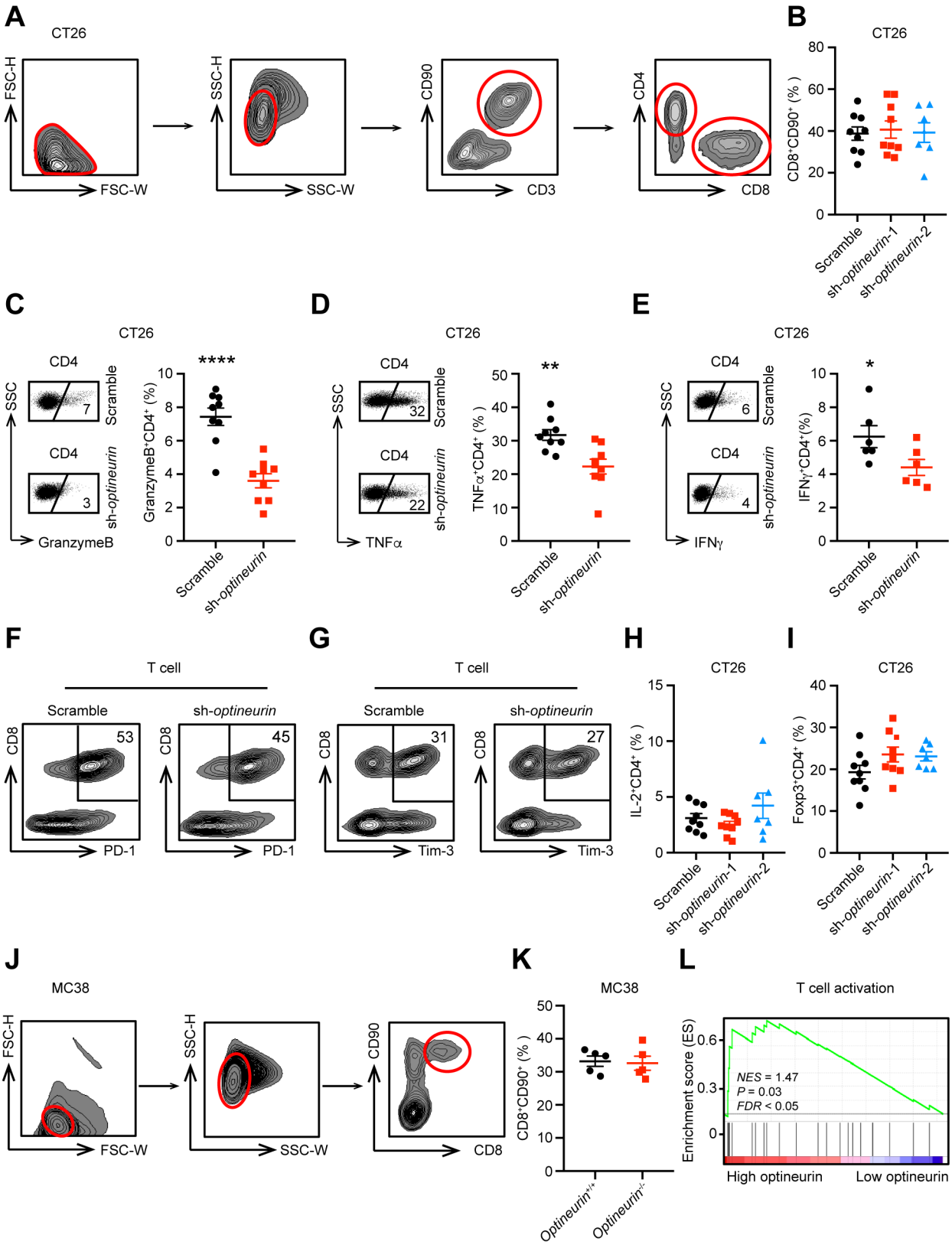

Supplementary Figure S4. Optineurin impacts cytotoxic T cell activation and function *in vivo*

A - I, Effect of tumor optineurin knocking down on tumor infiltrating T cells. sh-*optineurin* and scrambled shRNA expressing CT26 cells were inoculated into BALB/c mice. (**A**), Flow cytometry gating strategy determining different cell subsets in CT26 model. The percentages of tumor infiltrating $CD8^+$ cells (**B**), granzyme B^+CD4^+ T cells (**C**), $TNF\alpha^+CD4^+$ T cells (**D**), $IFN\gamma^+CD4^+$ T cells

(**E**), PD-1^{+}CD8^{+} T cells (**F**), Tim-3^{+}CD8^{+} T cells (**G**), IL-2^{+}CD4^{+} cells (**H**), and Foxp3^{+}CD4^{+} T cells (**I**) were analyzed by flow cytometry. Mean ± SEM, n = 7-9 /group. Scrambled shRNA vs. sh-*optineurin*, Two tailed t-tests, ****$P < 0.0001$, **$P < 0.001$, *$P < 0.001$.

J and **K,** Effect of tumor optineurin deficiency on MC38 tumor infiltrating T cell levels. *Optineurin*$^{+/+}$ and *optineurin*$^{-/-}$ expressing MC38 cells were inoculated into C57/BL6 mice. (**J**), Flow cytometry gating strategy determining different cell subsets in MC38 model. (**K**), The percentage of tumor infiltrating CD8^{+} T cells was analyzed by flow cytometry. Mean ± SEM, n = 5 /group. Two tailed t-tests. $P > 0.05$.

L, Correlation between optineurin protein expression and T cell activation signature in melanoma patients treated with anti-PD-1 therapy (n = 67).

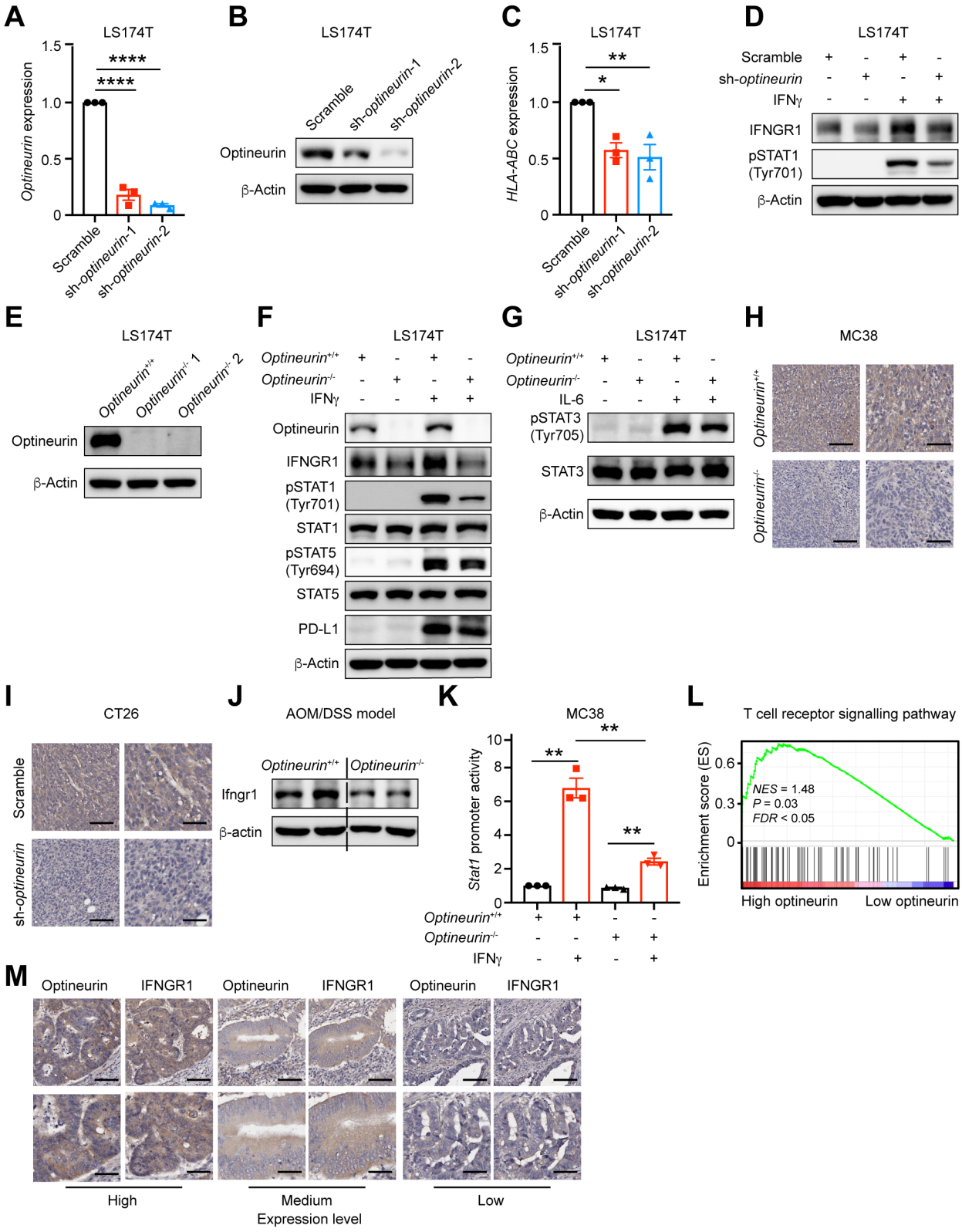

Supplementary Figure S5. Optineurin deficiency impairs IFNGR1 expression and antigen presentation

A and **B,** Optineurin knocking down efficiency in LS174T cells. (**A**) Optineurin was quantified by qRT-PCR in scramble and sh-*optineurin* expressing LS174T cells. n = 3, mean ± SEM. Two tailed t-tests, ****$P < 0.0001$. (**B**) Immunoblots analysis revealed optineurin expression in sh-*optineurin* (sh-*optineurin*-1 and sh-*optineurin*-2) and scrambled shRNA expressing LS174T cells. One of 3 repeats is shown.

C, Effect of sh-*optineurin* on *HLA-ABC* expression in LS174T cells. *HLA-ABC* was quantified by qRT-PCR in scramble and sh-*optineurin* expressing LS174T cells. n = 3, mean ± SEM. Two tailed t-tests, **P* < 0.05, ***P* < 0.01.

D - F, Effect of optineurin on the IFNγ pathway in LS174T cells. sh-*optineurin* LS174T cells (**D**) and optineurin knocked out (*optineurin*$^{-/-}$) LS174T cells (**E** and **F**) were stimulated with IFNγ (10 ng/ml) for 4 hours. Relevant proteins were determined by immunoblots. One of 3 repeats is shown.

G, Effect of optineurin on STAT3 in LS174T cells. *Optineurin*$^{+/+}$ and *optineurin*$^{-/-}$ LS174T cells were stimulated with IL-6 (20 ng/ml) for 30 minutes. pSTAT3 and STAT3 were determined by immunoblot. One of 3 repeats is shown.

H - J, Effect of optineurin on murine tumor Ifngr1 *in vivo*. Immunohistochemistry staining showed tumor tissue Ifngr1 expression in wild type mice bearing *optineurin*$^{-/-}$ MC38 (**H**), sh-*optineurin* CT26 (**I**), and control tumors. One of 5 mice/group is shown. Scale bars, (left) 100 μm, (right) 50 μm (magnified). (**J**) Immunoblots revealed Ifngr1 expression in *optineurin*$^{+/+}$ or *optineurin*$^{-/-}$ tumors in AOM/DSS murine model.

K, Effect of optineurin on *Stat1* promoter activity in MC38 tumor cells. *Stat1* reporter expressing *optineurin*$^{+/+}$ and *optineurin*$^{-/-}$ MC38 cells were stimulated with IFNγ for 4 hours. *Stat1* promoter activity is expressed as relative Renilla luciferase activity, normalized to unstimulated cells. n = 3, two tailed t-tests, ***P* < 0.01.

L, Correlation between optineurin protein expression and T cell receptor signaling signature in melanoma patients. T cell receptor signaling is enriched in high optineurin expression melanoma patients with anti-PD1 therapy (n = 67).

M, Correlation of optineurin expression with IFNGR1 expression in human colorectal cancer. Representative immunohistochemistry staining images showed high to low expression of optineurin and IFNGR1 expression in colorectal cancer tissues. Cohort 3, n = 78. Scale bars, (upper panels) 100 μm, (lower panels) 50 μm (magnified).

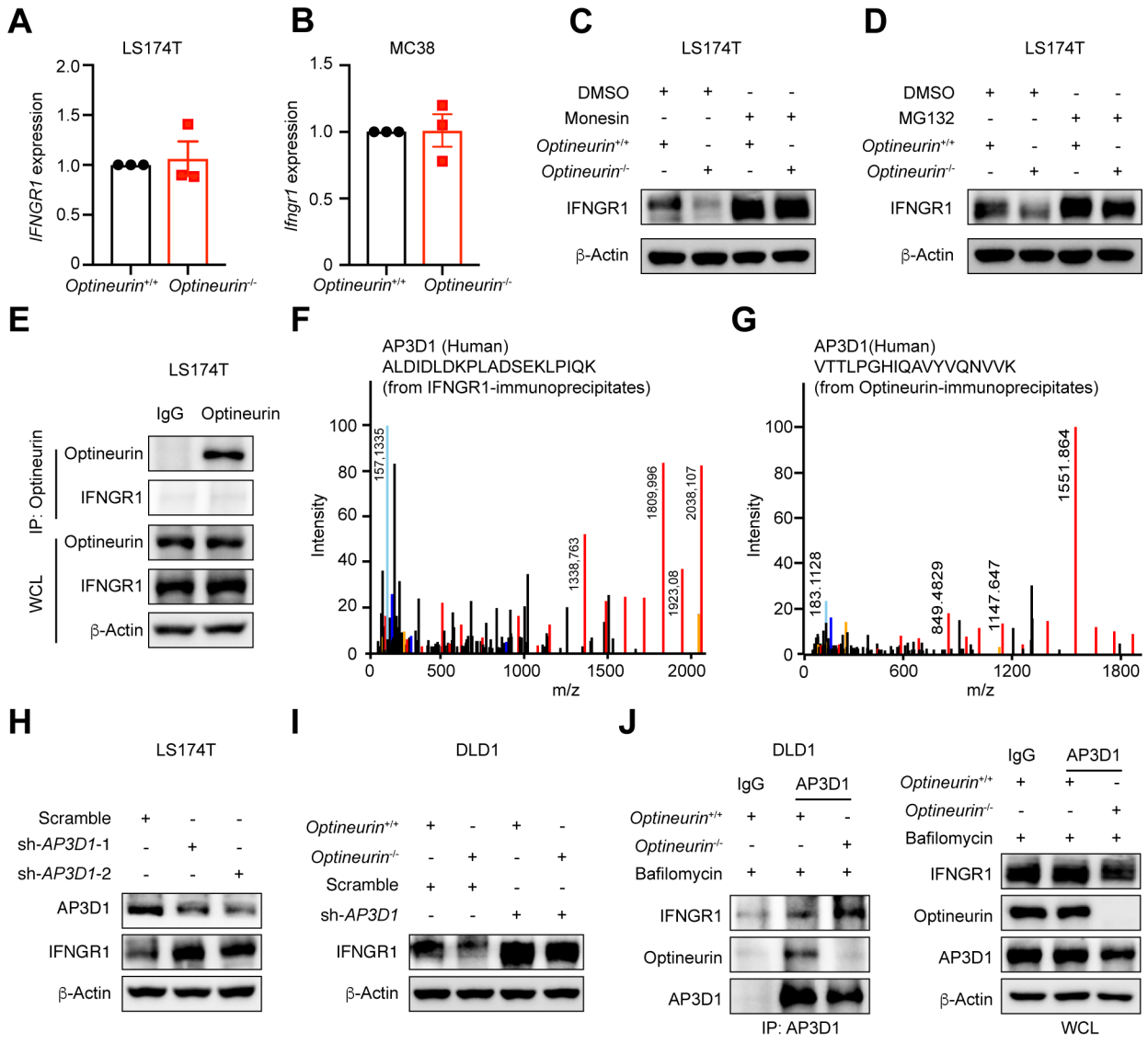

Supplementary Figure S6. Loss of optineurin promotes IFNGR1 lysosomal sorting via AP3D1

A and **B,** Effects of optineurin on *IFNGR1* transcripts. *IFNGR1* transcripts were quantified by qPCR in *optineurin*$^{+/+}$ and *optineurin*$^{-/-}$ LS174T cells (**A**) and MC38 cells (**B**), mean ± SEM, n = 3 biological replicates.

C, Effects of monensin on IFNGR1 expression. *Optineurin*$^{+/+}$ and *optineurin*$^{-/-}$ LS174T cells were treated with or without monensin for 4 hours. Immunoblots showed IFNGR1 expression. n = 3 biological replicates.

D, Effects of MG132 on IFNGR1 expression. *Optineurin*$^{+/+}$ and *optineurin*$^{-/-}$ LS174T cells were treated with or without MG132 for 4 hours. Immunoblots showed IFNGR1 expression. n = 3 biological replicates.

E, Detection of optineurin and IFNGR1 interaction. Proteins in LS174T cells were immunoprecipitated using anti-optineurin antibody and immunoblotted using anti-IFNGR1. WCL, whole-cell lysate. n = 3 biological replicates.

F and **G**, Representative spectrum of IP-MS. (**F**) Representative spectrum of unique peptides of AP3D1 in IFNGR1-immunoprecipitates. (**G**) Representative spectrum of unique peptides of AP3D1 in optineurin -immunoprecipitates.

H and **I**, Effect of sh-*AP3D1* on IFNGR1 expression. (**H**) Immunoblots showed AP3D1 and IFNGR1 expression in sh-*AP3D1* (sh-*AP3D1*-1 and sh-*AP3D1*-2) and scrambled shRNA expressing LS174T cells. One of 3 repeats is shown. (**I**) IFNGR1 expression in sh-*AP3D1* and scrambled shRNA expressing *optineurin*$^{+/+}$ and *optineurin*$^{-/-}$ LS174T cells. Immunoblots showed IFNGR1 expression. n = 3 biological replicates.

J, Effect of optineurin expression on the interaction between IFNGR1 and AP3D1. Detection of endogenous IFNGR1 and AP3D1 interaction by Co-IP. Proteins in *optineurin*$^{+/+}$ and *optineurin*$^{-/-}$ DLD1 cells were immunoprecipitated using anti-AP3D1 antibody and immunoblotted using anti-IFNGR1. Cells were treated with Bafilomycin for 4 hours. WCL, whole-cell lysate. n = 3 biological replicates.

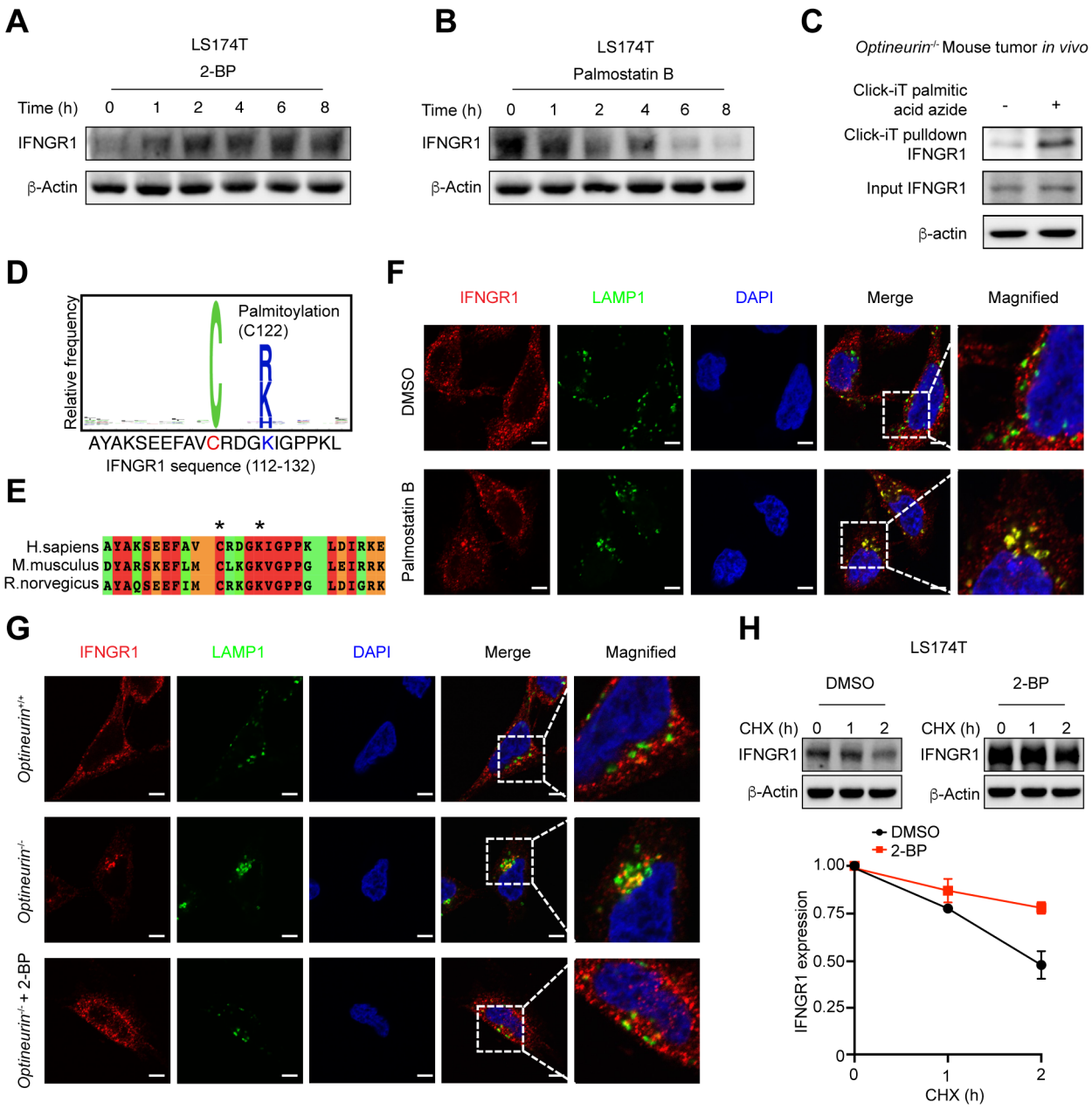

Supplementary Figure S7. IFNGR1 palmitoylation affects IFNGR1 lysosome degradation

A and **B,** Effect of 2-BP (**A**) and Palmostatin B (**B**) on IFNGR1 protein expression in LS174T cells. LS174T cells were treated with 2-BP (**A**) or Palmostatin B (**B**) for different time points. Immunoblots showed IFNGR1 protein expression. One of 3 replicates is shown.

C, Detection of IFNGR1 palmitoylation in *optineurin*$^{-/-}$ tumor cells *in vivo*. IECs were isolated from *optineurin*$^{-/-}$ mice in AOM/DSS models. IECs were treated and prepared for the Click-iT reaction. One of 3 repeats is shown.

D, Prediction of IFNGR1 palmitoylation at Cys122 by the MDD-Palm.

E, Palmitoylation site (Cys122) in different species.

F, Effect of Palmostatin B on tumor IFNGR1 lysosomal localization. DLD1 cells were treated with Palmostatin B and stained for IFNGR1 (Red) and LAMP1 (Green). Cell nucleus (Blue) was stained

DAPI. Representative immunofluorescence images showed the co-localization of IFNGR1 and LAMP1. Scale bars, 5 μm. n = 3 biological replicates.

G, Effect of 2-BP on tumor IFNGR1 lysosomal localization. *Optineurin*$^{-/-}$ and *Optineurin*$^{+/+}$ DLD1 cells were treated with 2-BP and stained for IFNGR1 (Red) and LAMP1 (Green). Cell nucleus (Blue) was stained DAPI. Representative immunofluorescence images showed the co-localization of IFNGR1 and LAMP1. Scale bars, 5 μm. n = 3 biological replicates.

H, Effect of palmitoylation on IFNGR1 stability. LS174T cells were treated with 2-BP in the presence of CHX. Immunoblots showed IFNGR1 protein expression bands (above) and intensities (bottom) at different time points. One of 3 replicates is shown.

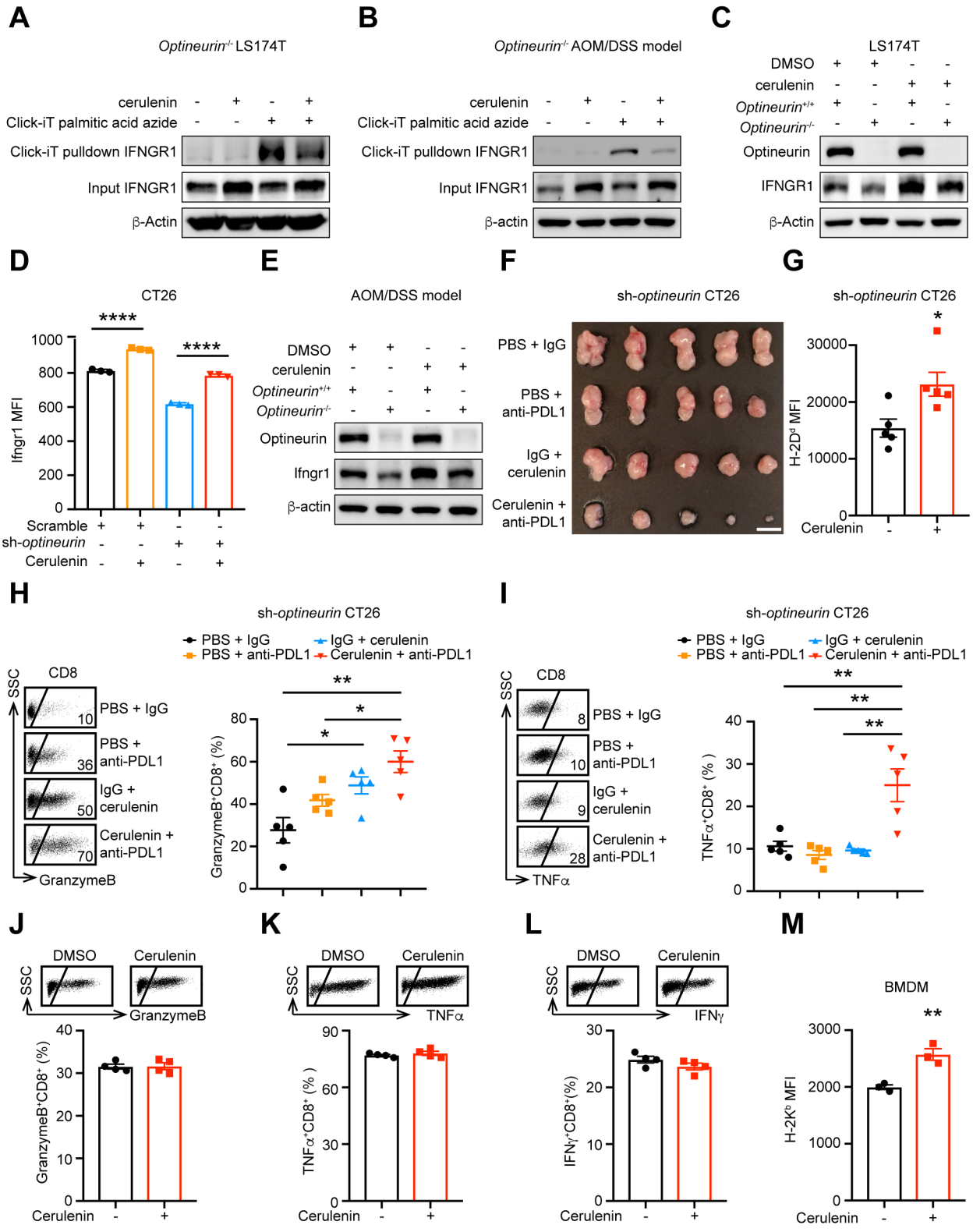

Supplementary Figure S8. Targeting IFNGR1 palmitoylation enhances immunotherapy efficacy

A and **B**, Effect of cerulenin on IFNGR1 palmitoylation. *Optineurin*$^{-/-}$ LS174T cells (**A**) and *optineurin*$^{-/-}$ IECs isolated from AOM/DSS murine models (**B**) were treated with cerulenin for 6 hours and prepared for the Click-iT reaction. One of 3 repeats is shown.

C - E, Effect of cerulenin on IFNGR1 expression. *Optineurin*$^{+/+}$ and *optineurin*$^{-/-}$ LS174T cells (**C**), scramble and sh-*optineurin* expressing CT26 cells (**D**), and *optineurin*$^{+/+}$ and *optineurin*$^{-/-}$ IECs

isolated from AOM/DSS murine models (**E**) were treated with cerulenin for 4 hours. IFNGR1 expression was detected by immunoblots (**C** and **E**) or flow cytometry (**D**). One of 3 repeats is shown.

F, Effect of cerulenin or combination with anti-PD-L1 therapy on sh-*optineurin* CT26 tumor progression. Tumor images are shown. Scale bars,1 cm.

G, Effect of cerulenin on $H2D^d$ expression in sh-*optineurin* CT26 tumor. The expression of $H\text{-}2D^d$ was analyzed by flow cytometry. Results are shown as mean fluorescence intensity (MFI). Mean ± SEM, n = 5 /group. Two tailed t-tests. $^*P < 0.05$.

H and **I,** Effect of cerulenin or combination with anti-PD-L1 therapy on sh-*optineurin* CT26 tumor infiltrating T cell function. Sh-*optineurin* CT26 cells were inoculated into BALB/c mice. Mice bearing Sh-*optineurin* CT26 tumor were treated with cerulenin, anti-PD-L1, or their combination. The percentages of tumor infiltrating granzyme B^+ (**H**) and $TNF\alpha^+$ (**I**) $CD8^+$ T cells were analyzed by flow cytometry. Mean ± SEM, n = 5 /group. Two tailed t-tests, $^*P < 0.05$, $^{**}P < 0.01$.

J - L, Effect of cerulenin on $CD8^+$ T cells. Splenocytes were stimulated with CD3 (2 μg/ml) and CD28 (1 μg/ml) for 3 days then treated with cerulenin (10 μM) for 4 hours. The percentages of granzyme B^+CD8^+ T cells (**J**), $TNF\alpha^+CD8^+$ T cells (**K**), $IFN\gamma^+CD8^+$ T cells (**L**) were analyzed by flow cytometry. Mean ± SEM, Two tailed t-tests, $P > 0.05$.

M, Effect of cerulenin on bone marrow derived macrophages. Bone marrow derived macrophages were treated with cerulenin (10 μM) for 4 hours. $H2K^b$ protein expression was determined by flow cytometry analysis. Results are shown as the mean fluorescence intensity (MFI) ± SEM. n = 3, Two tailed t-tests, $^{**}P < 0.01$

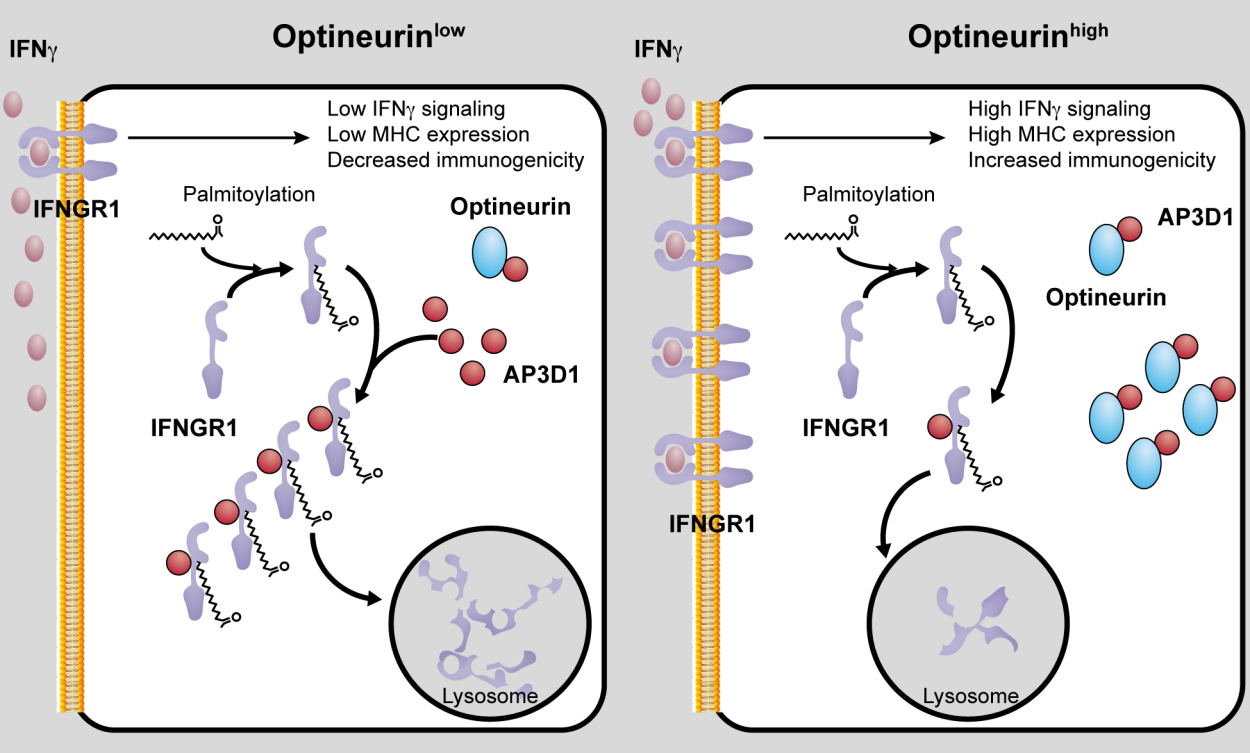

Supplementary Figure S9. Graphical model

AP3D1 interacts with and sorts palmitoylated-IFNGR1 to lysosome for degradation. Optineurin binds to AP3D1 to prevent palmitoylated-IFNGR1 lysosomal sorting and degradation. Loss of optineurin results in accelerated AP3D1-directed IFNGR1 lysosomal sorting and degradation, thereby impairing both IFNγ- and MHC-I-signaling integrity, abolishing tumor immunity, and endowing intrinsic immune resistance.

Supplementary Tables

Supplementary Table S1. Optineurin expression in paired colon cancer and adjacent normal colon tissues

Adjacent normal tissues	Adjacent optineurin	Cancer	Cancer optineurin
01CO005N	0.125	01CO005	-0.105
01CO006N	0.323	01CO006	-0.219
01CO008N	0.292	01CO008	-0.0643
01CO013N	0.0737	01CO013	-0.734
01CO014N	0.252	01CO014	-0.415
01CO015N	0.179	01CO015	-0.422
01CO019N	0.244	01CO019	-0.365
01CO022N	0.143	01CO022	-0.314
05CO002N	0.442	05CO002	-0.0639
05CO003N	0.149	05CO003	-0.499
05CO006N	0.225	05CO006	-0.0025
05CO011N	0.402	05CO011	-0.0486
05CO015N	0.101	05CO015	0.22
05CO020N	0.255	05CO020	-0.38
05CO026N	0.0189	05CO026	-0.269
05CO028N	0.493	05CO028	-0.49
05CO029N	0.29	05CO029	-0.0018
05CO032N	0.199	05CO032	0.0515
05CO033N	0.171	05CO033	0.268
05CO034N	-0.0371	05CO034	-0.106
05CO035N	0.306	05CO035	0.128
05CO037N	0.266	05CO037	-0.324
05CO039N	0.399	05CO039	-0.0082
05CO041N	0.32	05CO041	0.123
05CO044N	0.108	05CO044	-0.584
05CO045N	0.237	05CO045	0.0137
05CO047N	0.256	05CO047	-0.0713
05CO048N	0.135	05CO048	-0.486
05CO049N	-0.0817	05CO049	-0.376
05CO050N	0.274	05CO050	-0.743
05CO053N	0.294	05CO053	-0.462
05CO054N	0.213	05CO054	-0.279
06CO001N	0.421	06CO001	-0.226
06CO002N	0.495	06CO002	0.252
09CO005N	0.0783	09CO005	-0.117
09CO006N	0.315	09CO006	-0.241
09CO008N	0.409	09CO008	-0.326
09CO011N	0.0149	09CO011	0.0364
09CO013N	0.184	09CO013	-0.303

09CO014N	-0.0156	09CO014	-0.249
09CO015N	0.0501	09CO015	-0.154
09CO018N	0.21	09CO018	-0.269
09CO019N	-0.038	09CO019	0.337
09CO022N	-0.0683	09CO022	-0.545
11CO005N	0.511	11CO005	0.285
11CO007N	0.144	11CO007	0.0828
11CO008N	0.257	11CO008	0.254
11CO010N	0.392	11CO010	-0.198
11CO018N	0.312	11CO018	0.0658
11CO019N	0.0364	11CO019	-0.0316
11CO020N	0.268	11CO020	-0.251
11CO021N	0.493	11CO021	0.267
11CO022N	-0.0158	11CO022	0.0531
11CO027N	0.501	11CO027	0.156
11CO030N	0.575	11CO030	0.151
11CO031N	0.322	11CO031	0.179
11CO032N	0.449	11CO032	0.673
11CO033N	0.254	11CO033	0.294
11CO036N	0.381	11CO036	0.109
11CO037N	0.398	11CO037	0.241
11CO039N	0.421	11CO039	-0.435
11CO042N	0.0836	11CO042	-0.0686
11CO043N	0.276	11CO043	0.193
11CO044N	0.301	11CO044	-0.0138
11CO045N	0.135	11CO045	-0.023
11CO047N	0.196	11CO047	-0.164
11CO048N	0.0724	11CO048	0.137
11CO051N	0.0823	11CO051	0.105
11CO052N	0.232	11CO052	0.268
11CO053N	0.154	11CO053	0.173
11CO054N	0.185	11CO054	-0.403
11CO057N	0.322	11CO057	-0.0179
11CO058N	0.0375	11CO058	-0.0038
11CO061N	0.22	11CO061	-0.0493
11CO062N	0.553	11CO062	0.109
11CO070N	0.455	11CO070	-0.157
11CO072N	0.337	11CO072	0.56
11CO077N	0.195	11CO077	0.0617
11CO079N	0.111	11CO079	0.126
14CO005N	0.441	14CO005	-0.0507
15CO001N	0.301	15CO001	-0.269
15CO002N	0.199	15CO002	-0.282
16CO002N	0.315	16CO002	-0.54
16CO003N	0.354	16CO003	0.394
16CO006N	0.196	16CO006	-0.0339

16CO011N	0.367	16CO011	-0.409
20CO001N	0.218	20CO001	0.196
20CO003N	-0.173	20CO003	0.287
20CO004N	0.225	20CO004	-0.564
20CO006N	0.119	20CO006	-0.125
20CO007N	0.356	20CO007	-0.317
21CO006N	0.245	21CO006	0.0905
21CO007N	0.579	21CO007	-0.43
22CO004N	0.0143	22CO004	-0.125
22CO006N	0.439	22CO006	0.63
27CO004N	0.379	27CO004	-0.45

Supplementary Table S2. Expression of optineurin and patient outcome (cohort 1)

	Overall (Percentage)	HR (95% CI)	P
Age			
< 70	46.00	2.09 (1.22 – 3.60)	0.007
>= 70	54.00		
Gender			
Male	56.00	0.96 (0.57-1.61)	0.883
Female	44.00		
Stage			
I - II	61.00	2.62 (1.56 -4.40)	< 0.001
III - IV	39.00		
T stage			
T1 - T2	6.19	2.43 (0.59 – 9.96)	0.218
T3 - T4	93.81		
N stage			
N0	61.00	2.62 (1.56 – 4.40)	< 0.001
N1 - N3	39.00		
M stage			
M0	97.03	15.33 (4.23 -55.62)	< 0.001
M1	2.97		
Grade			
I - II	75.00	1.58 (0.89-2.79)	0.116
III	25.00		
Tumor localization			
Ascending colon	45.36		
Transverse colon	10.31	1.14 (0.50-2.59)	0.758
Descending colon	13.40	0.57 (0.24 -1.38)	0.215
Sigmoid colon	30.93	0.53 (0.28 – 1.00)	0.051
Optineurin			
Low (< median)	50.00	0.55 (0.32 – 0.95)	0.032
High (>= median)	50.00		

Supplementary Table S3. Expression of optineurin and IFNGR1 and patient outcome (cohort 3)

	Overall (Percentage)	HR (95%CI)	P
Age			
< 70	65.38	1.57 (0.50 - 4.97)	0.439
>= 70	34.62		
Gender			
Male	51.28	1 (0.32 - 3.09)	0.994
Female	48.72		
Stage			
I - II	52.56	NA	NA
III - IV	47.44		
T stage			
T1 - T2	36.84	2.88 (0.62 - 13.32)	0.177
T3 - T4	63.16		
N stage			
N0	66.22	1.18 (0.29 - 4.74)	0.814
N1 - N3	33.78		
M stage			
M0	62.82	NA	NA
M1	37.18		
Grade			
I - II	98.46	90.16 (5.41 - 1501.35)	0.002
III	1.54		
Tumor localization			
Colon	57.69	2.37 (0.75 - 7.50)	0.143
Rectum	42.31		
Optineurin			
Low (< median)	50.00	0.24 (0.07 - 0.91)	0.035
High (>= median)	50.00		
IFNGR1			
Low (< median)	50.00	0.24 (0.06 - 0.88)	0.032
High (>= median)	50.00		

Supplementary Table S4. Clinical and pathological characteristics of colorectal cancer patients (cohort 1)

	Optineurin		IFNGR1	
	Low (< median) (n = 46)	High (>= median) (n = 46)	Low (< median) (n = 45)	High (>= median) (n = 47)
Age				
< 70	21 (45.7%)	23 (50.0%)	21 (46.7%)	23 (48.9%)
>= 70	25 (54.3%)	22 (47.8%)	23 (51.1%)	24 (51.1%)
ND	0 (0%)	1 (2.2%)	1 (2.2%)	0 (0%)
Gender				
Male	19 (41.3%)	30 (65.2%)	19 (42.2%)	30 (63.8%)
Female	26 (56.5%)	16 (34.8%)	25 (55.6%)	17 (36.2%)
ND	1 (2.2%)	0 (0%)	1 (2.2%)	0 (0%)
Stage				
I - II	15 (32.6%)	39 (84.8%)	24 (53.3%)	30 (63.8%)
III - IV	30 (65.2%)	7 (15.2%)	21 (46.7%)	16 (34.0%)
ND	1 (2.2%)	0 (0%)	0 (0%)	1 (2.2%)
T stage				
T1 - T2	3 (6.5%)	3 (6.5%)	4 (8.9%)	2 (4.3%)
T3 - T4	40 (87.0%)	42 (91.3%)	39 (86.7%)	43 (91.5%)
ND	3 (6.5%)	1 (2.2%)	2 (4.4%)	2 (4.3%)
N stage				
N0	15 (32.6%)	39 (84.8%)	24 (53.3%)	30 (63.8%)
N1 – N3	30 (65.2%)	7 (15.2%)	21 (46.7%)	16 (34.0%)
ND	1 (2.2%)	0 (0%)	0 (0%)	1 (2.1%)
M stage				
M0	43 (93.5%)	46 (100%)	43 (95.6%)	46 (97.9%)
M1	3 (6.5%)	0 (0%)	2 (4.4%)	1 (2.1%)
Grade				
I - II	29 (63.0%)	40 (87.0%)	29 (64.4%)	40 (85.1%)
III	17 (37.0%)	6 (13.0%)	16 (35.6%)	7 (14.9%)
Tumor localization				
Ascending colon	24 (52.2%)	15 (32.6%)	21 (46.7%)	18 (38.3%)
Transverse colon	4 (8.7%)	6 (13.0%)	6 (13.3%)	4 (8.5%)
Descending colon	5 (10.9%)	7 (15.2%)	3 (6.7%)	9 (19.1%)
Sigmoid colon	12 (26.1%)	15 (32.6%)	13 (28.9%)	14 (29.8%)
ND	1 (2.2%)	3 (6.5%)	2 (4.4%)	2 (4.3%)

ND: No data

Supplementary Table S5. Clinical and pathological characteristics of colorectal cancer patients (cohort 3)

	Optineurin		IFNGR1	
	Low (< median) (n = 39)	High (>= median) (n = 39)	Low (< median) (n = 39)	High (>= median) (n = 39)
Age				
< 70	27 (69.2%)	24 (61.5%)	26 (66.7%)	25 (64.1%)
>= 70	12 (30.8%)	15 (38.5%)	13 (33.3%)	14 (35.9%)
Gender				
Male	18 (46.2%)	22 (56.4%)	20 (51.3%)	20 (51.3%)
Female	21 (53.8%)	17 (43.6%)	19 (48.7%)	19 (48.7%)
Stage				
I - II	9 (23.1%)	32 (82.1%)	8 (20.5%)	33 (84.6%)
III - IV	30 (76.9%)	7 (17.9%)	31 (79.5%)	6 (15.4%)
T stage				
T1 - T2	11 (28.2%)	17 (43.6%)	12 (30.8%)	16 (41%)
T3 - T4	26 (66.7%)	22 (56.4%)	25 (64.1%)	23 (59.0%)
ND	2 (5.1%)	0 (0%)	2 (5.1%)	0 (0%)
N stage				
N0	16 (41.0%)	33 (84.6%)	14 (35.9%)	35 (89.7%)
N1 - N3	19 (48.7%)	6 (15.4%)	21 (53.8%)	4 (10.3%)
ND	4 (10.3%)	0 (0%)	4 (10.3%)	0 (0%)
M stage				
M0	17 (43.6%)	32 (82.1%)	15 (38.5%)	34 (87.2%)
M1	22 (56.4%)	7 (17.9%)	24 (61.5%)	5 (12.8%)
Grade				
I - II	30 (76.9%)	34 (87.2%)	33 (84.6%)	31 (79.5%)
III	1 (2.6%)	0 (0%)	1 (2.6%)	0 (0%)
ND	8 (20.5%)	5 (12.8%)	5 (12.8%)	8 (20.5%)
Tumor localization				
Colon	20 (51.3%)	25 (64.1%)	22 (56.4%)	23 (59.0%)
Rectum	19 (48.7%)	14 (35.9%)	17 (43.6%)	16 (41.0%)

ND: No data

Supplementary Table S6. Identification of AP3D1 as binding partner for both IFNGR1 and optineurin

Identified Proteins	Description	Peptides	Protein ID
AP3D1	Adaptor protein complex AP-3 subunit delta-1	ALDIDLDKPLADSEKLPIQK (Both) GMELSVLDSLNAR (Both) LLESGDLSMSSIK (Both) LLESGDLSMSSIKVDGIR (Both) VTTLPGHIQAVYVQNVVK (Both)	O14617
AP3B1	Adaptor protein complex AP-3 subunit beta-1	LLDSITVPVAR (Both)	O00203
AP3M1	Adaptor protein complex AP-3 subunit mu-1	VLSFIPPDGNFR (Both) VSSQNLVAIPVYVK (Only optineurin)	Q9Y2T2

Supplementary Table S7. PCR primers

Target Gene	Forward primer	Reverse primer
Human *Optineurin*	ACTCTGACCAGCAGGCTTACCT	CTATGTCAGGCAGAACCTCTCC
Human *IFNGR1*	AGTGCTTAGCCTGGTATTCATCTG	GGCTGGTATGACGTGATGAGTG
Mouse *Ifngr1*	CTTGAACCCTGTCGTATGCTGG	TTGGTGCAGGAATCAGTCCAGG
Human *HLA-ABC*	CCTACGACGGCAAGGATTAC	TGCCAGGTCAGTGTGATCTC
Mouse *H2kb*	GGCAATGAGCAGAGTTTCCGAG	CCACTTCACAGCCAGAGATCAC
Human *β-Actin*	ATCCGCCGCCCGTCCACA	ACCATCACGCCCTGGTGCCT
Mouse *β-Actin*	CATTGCTGACAGGATGCAGAAGG	TGCTGGAAGGTGGACAGTGAGG
***IFNGR1* (C122A mutant)**	CAGAAGAATTTGCTGTAGCCCGAGATGGAAAAATTGG	CCAATTTTTCCATCTCGGGCTACAGCAAATTCTTCTG

Supplementary Table S8. MHC-I and IFN signaling signatures in colorectal cancer

MHC-I			IFN		
Gene	**logFC**	**P Value**	**Gene**	**logFC**	**P Value**
HLA.F	1.41395279	1.03E-75	*OAS2*	2.1278918	2.04E-100
HLA.B	1.11989186	1.28E-66	*IFIT3.x*	1.7414237	8.37E-97
HLA.A	0.95195055	2.24E-66	*RSAD2*	1.9709754	3.77E-85
HLA.E	0.74812381	1.13E-64	*IFI44L*	2.62901	7.04E-84
HLA.C	0.93116597	6.03E-62	*MX1*	1.8760285	1.63E-83
HCP5	1.15786853	3.16E-55	*PARP9*	1.0117091	8.49E-81
HLA.H	1.16147808	1.07E-50	*IFIT1*	2.0366698	1.34E-78
BTN3A3	0.88624856	3.22E-48	*DDX60*	1.3685832	5.22E-75
BTN3A1	0.78706868	1.16E-44	*IFI44*	1.726729	1.22E-74
PSMB9	1.04852593	4.34E-42	*DDX58*	1.0038025	2.28E-73
TAP1	0.9045302	1.22E-41	*IFIT2*	1.4383886	1.29E-69
PSMB8	0.58818543	4.38E-30	*CMPK2*	1.4741036	8.01E-69
BTN3A2	0.62749689	5.32E-30	*STAT1*	1.0909087	1.65E-64
BTN2A2	0.5480004	9.63E-30	*SAMD9L*	1.4622512	5.09E-61
NLRC5	0.74607379	1.37E-27	*PARP14*	0.9268966	2.67E-60
HLA.G	1.13049148	6.09E-26	*IFI6*	1.7698809	7.64E-60
HCG4P11	1.35176457	7.09E-26	*OAS3*	1.0768439	4.60E-58
CD74	0.97184214	1.28E-25	*GBP1*	1.3194004	9.16E-57
TAP2	0.6014486	1.30E-25	*ISG15*	1.4550293	1.06E-54
HLA.DMA	0.92259965	4.19E-25	*UBE2L6*	1.1257711	5.49E-53
UBE2L6	0.79002411	1.22E-24	*IFIH1*	0.8684	1.84E-51
ETV7	0.85524514	4.20E-24	*XAF1*	1.3023888	1.87E-51
IRF1	0.65771391	5.70E-24	*GBP4*	1.6669084	1.04E-50
APOL3	0.85108386	9.27E-23	*CXCL10*	2.1187915	2.30E-50
HLA.DMB	0.95815719	5.41E-22	*SAMHD1*	0.8376622	2.90E-49
CCL5	1.04185253	1.19E-21	*SP100*	0.6115045	1.36E-48
IL15RA	0.47758457	2.68E-21	*IFIT5*	0.8203921	1.38E-48
HCST	0.83117101	8.19E-21	*HERC6*	0.940609	1.87E-48
PSMB10	0.54776622	1.90E-20	*SAMD9*	1.3109065	7.59E-48
HLA.DRA	1.05065499	2.67E-20	*BST2*	1.7349855	1.46E-47
SLC15A3	0.74549187	2.73E-20	*TYMP*	1.301277	4.36E-47
RARRES3	1.05181993	5.39E-20	*CD74*	1.2787447	2.27E-46
C10orf54	0.54659649	5.94E-20	*USP18*	1.1410467	8.84E-46
HLA.DRB1	0.97631288	9.05E-20	*SLC15A3*	1.0934439	1.22E-45
WAS	0.68726469	9.43E-20	*HLA.DRA*	1.5316293	4.39E-45
HLA.DPB1	0.95230556	1.26E-19	*MX2*	1.1168286	7.47E-45
GBP2	0.67423941	1.92E-19	*LAP3*	0.636091	1.51E-44
APOL2	0.59462517	2.02E-19	*TRIM22*	1.1956043	7.74E-44
CD72	0.64160096	2.16E-19	*STAT2*	0.6777948	8.99E-44
IL12RB1	0.81118451	3.00E-19	*RARRES3*	1.5311107	2.34E-42
GBP4	1.0176423	1.66E-18	*HLA.DMB*	1.3032155	8.42E-42
HLA.DPA1	1.03312875	2.98E-18	*HLA.DRB1*	1.3874786	3.04E-41
SELPLG	0.70913472	3.00E-18	*TAP1*	0.8994499	7.56E-41

FGD2	0.63334719	3.51E-18
AIM2	1.37507152	3.77E-18
SASH3	0.72714237	3.83E-18
PGLYRP2	1.23553398	4.54E-18
PSTPIP1	0.5986463	7.94E-18
HLA.DRB5	1.11329801	8.58E-18
HLA.J	0.95078129	8.79E-18
OR2I1P	1.27046255	1.05E-17
TAPBP	0.40632825	1.15E-17
ICAM1	0.68222822	1.31E-17
TYMP	0.8102277	1.35E-17
CD52	0.77546715	1.49E-17
SECTM1	0.93442251	1.54E-17
CSF1	0.56542783	2.18E-17
THEMIS2	0.61553029	3.65E-17
PIK3CD	0.64353516	4.78E-17
HLA.W	0.89734245	6.56E-17
GBP1	0.7416352	6.61E-17
TRANK1	0.53184449	6.85E-17
CIITA	0.9333822	7.12E-17
UBA7	0.49200695	7.37E-17
CYTH4	0.70189773	7.89E-17
IL16	0.67830506	8.49E-17
NKG7	0.94504606	8.57E-17
DOK2	0.69882779	9.57E-17
C19orf38	0.75335635	1.45E-16
UBASH3A	0.75785582	1.47E-16
MYO1G	0.67935379	1.49E-16
LSP1	0.68311528	1.61E-16
ARHGAP9	0.65459981	1.64E-16
ITGAL	0.76619369	2.21E-16
X1.Sep	0.54182578	2.33E-16
CD37	0.77064175	3.20E-16
CD3E	0.77379643	3.69E-16
ODF3B	0.68543837	4.92E-16
HLA.L	1.17532922	6.44E-16
IL2RB	0.74600526	6.84E-16
NCF1	0.80982987	7.29E-16
TRAC	0.70797164	7.72E-16
CD82	0.45660214	7.77E-16
HLA.DOA	0.93798682	9.47E-16
TRBC2	0.76758292	1.00E-15
SLAMF8	0.77558	1.09E-15
SPI1	0.70404976	1.11E-15
FMNL1	0.57789279	1.24E-15
HCG4P7	0.90256594	1.34E-15
SLA	0.69422719	1.36E-15
CXCL11	2.1295744	1.33E-40
SIGLEC1	1.52915	1.34E-40
GBP1P1	1.6348309	1.63E-40
TNFSF13B	1.2907711	4.36E-40
GBP5	1.6653661	4.83E-40
HLA.DPA1	1.5050897	4.97E-40
TRIM69	0.7121708	8.14E-40
ICAM1	1.0142351	8.91E-40
CCL8	2.00921	2.76E-39
HLA.E	0.6057793	3.35E-39
CCL5	1.3956512	5.05E-39
HLA.DPB1	1.322839	6.16E-39
HAVCR2	1.1760946	6.81E-39
CD86	1.1712036	2.95E-38
OASL	1.2161407	2.98E-38
CXCL9	1.9490192	3.27E-38
CD274	1.2257661	3.56E-38
HAPLN3	1.1215236	3.75E-38
SLAMF8	1.2019697	5.73E-38
IRF1	0.8198886	8.37E-38
HLA.DMA	1.1273233	9.20E-38
APOL2	0.8191343	1.73E-37
APOL3	1.0876545	2.19E-37
CCR5	1.1146164	2.24E-37
C1QA	1.2033372	2.79E-37
LAPTM5	1.1583502	3.10E-37
FCGR3A	1.5654871	4.85E-37
CTSL	1.0066749	5.05E-37
CD53	1.2019207	8.01E-37
BTN3A3	0.7798623	3.99E-36
PDCD1LG2	1.3851532	4.92E-36
APOL6	0.7072961	5.63E-36
IRF7	0.8391317	8.36E-36
LILRB4	1.3840015	9.87E-36
FPR3	1.3059659	1.42E-35
CCR1	1.0608624	1.50E-35
IDO1	2.0078862	1.60E-35
TIGIT	1.2911599	1.69E-35
GIMAP4	0.8972588	1.70E-35
BTK	1.0570068	1.94E-35
FCER1G	1.1107733	3.27E-35
IFI16	1.0856596	3.31E-35
SCIMP	1.0945375	4.34E-35
SLA	1.0367688	4.90E-35
LCP2	0.9992386	8.47E-35
AIF1	0.9121684	1.25E-34
LSP1	0.9816263	1.93E-34

IL18BP	0.51421398	1.46E-15
MYO1F	0.56290592	1.47E-15
IFNG	1.31428876	1.48E-15
ARHGAP30	0.65975683	1.73E-15
TBC1D10C	0.69574399	1.97E-15
CD53	0.78028838	2.23E-15
IFIT3.x	0.74574077	2.40E-15
HLA.DOB	0.80599357	3.13E-15
XAF1	0.71841463	3.14E-15
TNFAIP8L2	0.55668354	3.66E-15
GPSM3	0.47793669	3.71E-15
RASAL3	0.59551738	3.92E-15
CD247	0.65089733	3.98E-15
CD274	0.76564316	4.68E-15
IKZF1	0.74178146	4.97E-15
SAMD9L	0.74742767	5.84E-15
NCF1C	0.79984394	6.65E-15
HCG4P5	1.1873953	7.52E-15
RHOH	0.7083411	8.07E-15
S1PR4	0.7480271	8.90E-15
HCG4	1.09318699	9.82E-15
IDO1	1.25941709	1.04E-14
LGALS9	0.47137635	1.19E-14
CD8A.x	0.90676255	1.23E-14
CCR5	0.69852089	1.39E-14
C1QC	0.80566829	1.53E-14
LY9	0.86495139	1.78E-14
IL21R	0.73959353	1.90E-14
NAGK	0.27956283	1.98E-14
NCR3	0.9271683	1.99E-14
HCLS1	0.6021989	2.14E-14
STX11	0.71093502	2.16E-14
APOL1	0.74244153	2.32E-14
PARP9	0.45502699	2.55E-14
TBX21	0.89461309	2.65E-14
LILRB1	0.69727365	2.78E-14
DOK3	0.5170499	2.82E-14
FAM78A	0.53221868	3.04E-14
MAP4K1	0.63091782	3.10E-14
C1QA	0.74492853	3.28E-14
GBP5	0.98886274	3.42E-14
PIK3R5	0.65555925	3.44E-14
TNFSF14	0.70970737	3.64E-14
IL10RA	0.68003415	3.83E-14
LGALS12	1.17023084	4.22E-14
CXCL10	1.11929198	4.40E-14
HLA.DQA1	0.89079606	4.96E-14
SRGN	1.1963829	2.14E-34
HERC5	1.0874062	2.65E-34
MNDA	1.2709011	3.51E-34
HCLS1	0.924002	7.46E-34
TNFRSF9	1.0557868	1.14E-33
APOL1	1.1375466	1.28E-33
CD84	1.2724908	1.29E-33
APOBEC3G	1.0134096	1.48E-33
RASGRP3	0.7401237	1.49E-33
CYBB	1.2128209	1.57E-33
APBB1IP	1.0224296	2.07E-33
PLEK	1.3109973	2.40E-33
PTPRC	1.2748392	3.42E-33
NCF2	1.1535536	3.49E-33
IFI27	0.9685636	3.56E-33
KLRD1	1.526663	3.76E-33
CCL7	2.0293256	3.78E-33
MAFB	1.1024796	4.96E-33
TFEC	1.2599907	5.31E-33
EPSTI1	1.0328322	6.76E-33
SPI1	1.0121745	6.97E-33
CIITA	1.3122952	6.99E-33
P2RX7	1.0185949	7.55E-33
ITGB2	1.2519397	7.86E-33
PARVG	0.86124	8.02E-33
LCP1	1.1393391	8.52E-33
IL10RA	1.0364916	9.09E-33
C1QB	1.241905	9.32E-33
FYB	1.1278421	1.01E-32
IFI35	0.6482235	1.09E-32
LAIR1	1.0279054	1.31E-32
ITGAL	1.0767168	1.88E-32
PSMB9	0.9310368	2.10E-32
PLA2G7	1.0000362	2.33E-32
CLEC7A	1.1464567	2.33E-32
TYROBP	1.1213219	2.69E-32
ARHGAP25	0.7745632	2.77E-32
PARP12	0.5875101	3.70E-32
GPNMB	1.4733626	3.90E-32
C1QC	1.1883976	4.39E-32
ICOS	1.1557355	6.39E-32
CYTH4	0.960559	6.91E-32
C1orf162	0.8378315	9.92E-32
SERPING1	1.1446513	1.10E-31
SECTM1	1.2675619	1.36E-31
TRAC	0.9973453	1.47E-31
WARS	0.8045897	1.58E-31

TTC7A	0.32287521	5.14E-14
HAPLN3	0.68095495	5.21E-14
LAPTM5	0.71271332	5.67E-14
CD14	0.67024362	6.02E-14
UBD	1.08952608	6.15E-14
GBA	0.289047	6.52E-14
FTH1P22	1.01402828	6.61E-14
LAIR1	0.6696334	7.16E-14
TYROBP	0.73484349	7.24E-14
DPYD	0.76634049	7.38E-14
CD48	0.72531308	7.62E-14
NFAM1	0.55272913	7.90E-14
SIGLEC10	0.67973467	8.11E-14
LAG3	0.7513369	8.18E-14
APOBEC3G	0.64525215	8.93E-14
GZMH	0.93375817	9.38E-14
DNASE2	0.28744351	9.61E-14
ACAP1	0.5555768	9.68E-14
GIMAP1	0.48559905	9.83E-14
PARP12	0.38338549	1.04E-13
APOL4	0.71003755	1.05E-13
C16orf54	0.83565853	1.10E-13
IFI35	0.41595202	1.22E-13
BAK1	0.3556199	1.26E-13
NCF1B	0.8385355	1.33E-13
DOCK2	0.70800961	1.40E-13
ZMYND15	0.52124524	1.41E-13
ARHGAP25	0.49961562	1.41E-13
CD300A	0.64970949	1.48E-13
SERPINB9	0.41100204	1.81E-13
C5orf56	0.42876066	1.94E-13
C19orf66	0.34408271	2.08E-13
PLCG2	0.59047173	2.48E-13
ITGB2	0.79534764	2.63E-13
IL2RA	0.73465817	2.64E-13
PIK3AP1	0.63678251	2.66E-13
IL15	0.55920193	2.88E-13
ABI3	0.47801751	3.16E-13
CXCL9	1.12947569	3.39E-13
PLD3	0.32542459	3.39E-13
APBB1IP	0.63976498	3.54E-13
PTAFR	0.68398636	3.80E-13
CD96	0.71086902	3.83E-13
NFKB2	0.34949584	4.23E-13
CCL4	0.75379265	4.44E-13
CD6	0.52308644	4.50E-13
PDCD1	0.75815387	4.68E-13
SASH3	0.9507234	1.67E-31
IL21R	1.0888747	2.78E-31
CSF1	0.7550573	3.54E-31
IL2RB	1.0453769	3.79E-31
SAMSN1	1.03099	3.93E-31
PLEKHO1	0.783612	4.13E-31
SP110	0.6710954	4.57E-31
AIM2	1.7961536	4.92E-31
EVI2B	1.0688043	5.13E-31
APOE	1.5838597	5.56E-31
HLA.DOA	1.316145	6.38E-31
DOCK2	1.0699124	7.01E-31
CMKLR1	1.024963	7.14E-31
DOK2	0.9432319	7.24E-31
NCKAP1L	1.0070582	8.20E-31
CD48	1.0876547	8.55E-31
EVI2A	1.130619	9.01E-31
CXCL13	2.0593042	9.29E-31
CD2	1.072725	9.80E-31
DTX3L	0.4817284	1.95E-30
HLA.DQA1	1.3196942	2.30E-30
CLEC2B	0.916651	2.64E-30
ITGAX	1.0793918	2.76E-30
ARHGAP30	0.922061	3.90E-30
WAS	0.8416857	4.09E-30
NCF1	1.1071425	4.42E-30
PIK3AP1	0.9626182	5.06E-30
CD4	0.9751464	5.08E-30
STX11	1.0257135	6.52E-30
IFNG	1.8116835	7.22E-30
CD300LF	1.0294615	7.28E-30
HCK	0.973237	7.77E-30
IKZF1	1.0468105	8.01E-30
FMNL1	0.7968507	8.57E-30
HLA.DRB5	1.4372355	9.96E-30
KLHDC7B	1.1544733	1.52E-29
LILRB1	1.0008839	1.86E-29
SP140	1.0724756	1.91E-29
CLIC2	0.8876525	1.92E-29
C3AR1	1.1088383	1.92E-29
TAP2	0.6441243	1.98E-29
DDX60L	0.7511187	2.00E-29
CFH	1.0255214	2.02E-29
FAM78A	0.7645611	2.35E-29
LY96	1.0470307	2.40E-29
PLXNC1	0.9244453	2.70E-29
FGR	1.0009896	2.88E-29

SLA2	0.60742887	4.90E-13
CTSD	0.36273595	4.97E-13
TAGAP	0.6605007	5.03E-13
GZMM	0.75035822	5.11E-13
SMAP2	0.28814693	5.16E-13
LRRC25	0.62485415	5.68E-13
STAT1	0.50434403	6.54E-13
NCKAP1L	0.64725603	6.56E-13
ICAM3	0.77292754	6.75E-13
TTC24	1.06311726	6.99E-13
GMFG	0.46738678	7.20E-13
PDE6G	0.67818334	7.27E-13
TIGIT	0.77294027	7.57E-13
CD2	0.68679769	7.63E-13
EPSTI1	0.64604294	7.80E-13
HK3	0.80339002	7.91E-13
PATL2	0.56217278	8.01E-13
TNFSF12	0.43712046	8.40E-13
LILRP2	0.99594329	8.64E-13
C1QB	0.77345184	9.06E-13
TRIM22	0.65209018	9.17E-13
MMP25	0.61676565	9.62E-13
HLA.DQB1	0.88807156	9.77E-13
ISG20	0.55508838	9.83E-13
CD4	0.63041178	1.00E-12
TNFSF13B	0.72555793	1.15E-12
TRIM69	0.40118022	1.18E-12
OPTN	0.3305723	1.26E-12
TRPV2	0.50442462	1.28E-12
B2M	0.44444316	1.29E-12
CMKLR1	0.65021586	1.33E-12
HCK	0.62663708	1.33E-12
LTB	0.60191371	1.35E-12
LILRB4	0.81520664	1.43E-12
CD3D	0.68855111	1.46E-12
PLEKHO1	0.49111878	1.66E-12
CYLD	0.30005183	1.73E-12
FCGR1B	0.90996809	1.80E-12
SIRPG	0.72845242	2.06E-12
CD27	0.73747078	2.28E-12
OSCAR	0.62939371	2.45E-12
NECAP2	0.23301409	2.47E-12
APOL6	0.41188568	2.54E-12
CD7	0.75931519	2.56E-12
ZNF831	0.83672099	2.63E-12
FCRL6	0.93126858	2.92E-12
SPHK1	0.73802297	2.95E-12
CFAP54	1.3616306	3.15E-29
FCGR2B	1.2907038	3.50E-29
CLEC4E	1.5762067	4.11E-29
CCL18	2.083036	5.01E-29
SIRPB2	1.0628283	5.31E-29
SIGLEC10	0.9884963	5.58E-29
CD8A.x	1.2822558	6.48E-29
DPYD	1.1176218	7.66E-29
IL18BP	0.6985967	1.14E-28
PTAFR	1.0189394	1.23E-28
HLA.C	0.6628439	1.49E-28
LINC01094	1.1506033	1.50E-28
B2M	0.6750197	1.55E-28
FAM49A	0.8885245	1.62E-28
KLHL6	1.0184289	2.08E-28
TRAF3IP3	0.8790504	2.08E-28
GBP2	0.8175169	2.09E-28
CD96	1.0549302	2.25E-28
IL2RA	1.0758554	2.82E-28
TAGAP	0.9841592	3.06E-28
UBD	1.5690611	3.35E-28
CD163	1.4035086	3.43E-28
BCL2A1	1.1803274	3.69E-28
CD37	1.0125128	3.74E-28
MS4A6A	1.0132819	5.10E-28
FCGR1A	1.1915489	5.73E-28
HK3	1.1945965	5.89E-28
FBXO39	1.5825086	6.07E-28
CCL4	1.1190776	6.10E-28
ZBP1	1.0299782	6.80E-28
TLR8	1.4731737	7.11E-28
ARHGAP9	0.8488676	7.24E-28
SLA2	0.892866	9.02E-28
BIRC3	0.9565167	1.05E-27
SELL	1.1846846	1.21E-27
RAB31	1.0786655	1.25E-27
MILR1	0.9129278	1.33E-27
FCGR1B	1.4029407	1.43E-27
DOCK10	0.7984822	1.79E-27
TNFAIP8L2	0.7465295	2.14E-27
LY86	0.8628396	2.48E-27
ZBED2	1.5948424	2.67E-27
PRRX1	1.2814153	3.08E-27
MS4A4A	1.1388272	3.13E-27
CECR1	1.0698545	3.36E-27
IL4I1	1.058935	3.73E-27
EVL	0.7609113	4.71E-27

CPNE5	0.5378604	3.13E-12
KLHL6	0.66105011	3.25E-12
TRGC1	0.93126658	3.29E-12
RTP4	0.56750876	3.64E-12
DTHD1	1.07389803	3.70E-12
STK10	0.27974621	3.70E-12
LINC01127	1.09035204	3.91E-12
FGR	0.63982474	3.97E-12
CXCR6	0.66715226	4.28E-12
WDFY4	0.67585354	4.43E-12
LILRA4	0.99269086	4.65E-12
WARS	0.48883879	4.72E-12
TRAF3IP3	0.56449958	4.90E-12
CSF2RB	0.69225302	4.91E-12
LCP2	0.58113476	5.06E-12
TRBV28	0.63608916	5.19E-12
CYTIP	0.59843058	5.76E-12
SP140	0.67278003	6.22E-12
ALOX5	0.7187294	6.34E-12
LST1	0.5560818	6.34E-12
PARP14	0.42192903	6.37E-12
LILRB2	0.6533345	6.51E-12
C1orf162	0.50330963	7.44E-12
PRF1	0.75003358	7.82E-12
GZMK	1.03085717	8.55E-12
MGAT1	0.25465211	8.63E-12
CD3G	0.64483955	8.95E-12
PARVG	0.50959207	9.62E-12
RSAD2	0.76687682	1.04E-11
C10orf128	0.53680046	1.05E-11
PPM1M	0.36976938	1.08E-11
SIGLEC9	0.65499154	1.10E-11
CD84	0.7391745	1.14E-11
PTPRC	0.74617998	1.20E-11
SYTL3	0.34292483	1.30E-11
MOB3C	0.23760731	1.30E-11
ALOX5AP	0.58933619	1.31E-11
ZBP1	0.65280098	1.32E-11
CMPK2	0.61929636	1.38E-11
SLAMF7	0.84269969	1.44E-11
HLA.DRB9	0.95466549	1.69E-11
PIK3R6	0.49800679	1.70E-11
SIGLEC7	0.71800658	1.72E-11
HAVCR2	0.63158047	1.79E-11
RCSD1	0.48037697	1.79E-11
ACP2	0.25660618	1.81E-11
METRNL	0.47313832	1.82E-11
IGSF6	0.8836736	5.76E-27
SLC1A3	1.304052	6.52E-27
NKG7	1.1986089	7.24E-27
LAG3	1.0576687	7.68E-27
LILRB2	0.9883477	8.26E-27
BTN3A1	0.6239614	8.66E-27
ARHGEF6	0.7561998	9.05E-27
CRTAM	1.5127563	9.25E-27
SLAMF7	1.3011973	9.70E-27
VCAM1	0.9180585	1.19E-26
UBASH3B	0.9418917	1.22E-26
TRPV2	0.7347795	1.34E-26
CSF2RB	1.0412905	1.44E-26
GNB4	0.8307823	1.65E-26
TNFAIP2	0.909861	1.68E-26
CD3E	0.9918332	1.83E-26
GM2A	0.4515723	1.84E-26
TRAV16	1.4714864	2.35E-26
ARHGAP15	0.6830484	3.31E-26
PIK3R5	0.892219	3.52E-26
C10orf128	0.8133912	3.61E-26
RHOH	0.9450081	3.70E-26
FAM20A	0.9508305	3.70E-26
CLIP4	0.9977192	3.78E-26
MSR1	1.3519812	3.87E-26
IL16	0.8440688	4.10E-26
CD14	0.9225798	4.45E-26
CYLD	0.4384488	4.62E-26
CHST11	0.8562295	4.63E-26
FCGR2A	0.9681811	4.91E-26
GMFG	0.6697768	6.79E-26
SH2D1A	1.2271835	6.80E-26
IFNL1	1.0089261	7.93E-26
ADAMTS2	1.1777224	8.03E-26
TBX21	1.2068352	1.06E-25
ITGAM	1.1638767	1.13E-25
MYO1F	0.7236866	1.17E-25
LILRA4	1.4908125	1.19E-25
PLEKHO2	0.6639709	1.26E-25
LTA	0.9662746	1.32E-25
RASSF5	0.7624376	1.43E-25
CD52	0.9370939	1.52E-25
GZMK	1.5339412	1.52E-25
PPP1R18	0.6782049	1.58E-25
FGL2	1.0348971	1.80E-25
KMO	0.8996104	1.82E-25
PILRA	0.966833	1.86E-25

SLAMF1	0.60114124	1.83E-11
XCL2	0.95984388	1.87E-11
DDX58	0.41234648	1.91E-11
CORO1A	0.51129796	1.95E-11
CTSW	0.84297902	2.10E-11
JAK3	0.45302291	2.13E-11
GZMA	0.78189705	2.16E-11
LTA	0.6343675	2.31E-11
ITK	0.66324419	2.43E-11
RAB33A	0.51512685	2.56E-11
SPOCK2	0.57864329	2.57E-11
NLRC3	0.43839888	2.57E-11
TRGV10	0.98742497	2.63E-11
GBP1P1	0.8607521	2.65E-11
PINK1	0.34476198	2.79E-11
TCN2	0.47532775	2.80E-11
GM2A	0.28940685	2.83E-11
IFI16	0.61010256	2.91E-11
HCG4P3	0.67349308	2.99E-11
TAPBPL	0.40212963	3.03E-11
ITGAM	0.75806249	3.13E-11
CD22	0.87194968	3.43E-11
SIGLEC1	0.80364436	3.48E-11
MAFB	0.63539445	3.51E-11
TRIM21	0.26811782	3.57E-11
NAPSB	0.60742115	3.66E-11
DOCK8	0.58492002	3.70E-11
ZNF683	1.06982835	3.75E-11
SLC2A5	0.68323725	3.76E-11
SH2D1A	0.79328435	3.85E-11
CD86	0.62496427	3.86E-11
SRGN	0.67075339	3.89E-11
SCIMP	0.60947834	4.10E-11
CHI3L2	0.80927712	4.54E-11
IFI27	0.55533983	4.68E-11
CLEC17A	0.98625131	4.81E-11
VAMP5	0.50982901	4.94E-11
PLEK	0.73966135	5.06E-11
MR1	0.42389299	5.07E-11
PHF1	0.2940166	5.93E-11
HLA.DRB6	0.926833	6.92E-11
CD300LF	0.61222871	6.93E-11
FCER2	1.10555212	7.43E-11
FAM26F	0.73428893	7.52E-11
IL4I1	0.65842145	7.76E-11
GIMAP6	0.50646764	7.77E-11
GIMAP7	0.47169419	7.93E-11
MAF	0.7692175	2.05E-25
GPR68	0.8485549	2.12E-25
MYO1G	0.8363788	2.15E-25
CCL2	1.0461736	2.23E-25
APOBEC3A	1.2700266	2.40E-25
KCND2	1.7332523	2.45E-25
TLR1	1.0084354	2.59E-25
LST1	0.8181477	2.72E-25
PIP4K2A	0.4230535	3.39E-25
PIK3CD	0.781936	3.49E-25
VIM	0.8152021	4.17E-25
PYHIN1	1.1521564	4.39E-25
CD300A	0.8865489	4.42E-25
ISG20	0.785566	6.19E-25
CD226	1.0327471	7.34E-25
GIMAP7	0.7306876	7.53E-25
CD80	1.0057045	8.08E-25
CD3G	0.9498045	8.19E-25
ITK	0.9958529	9.09E-25
SIGLEC9	0.9588672	9.18E-25
ACP5	0.8551427	1.72E-24
HCST	0.8991903	1.85E-24
LINC00968	1.4474892	1.88E-24
LRRC25	0.8589517	1.89E-24
OR2I1P	1.4938964	2.09E-24
CLEC4A	0.7794098	2.47E-24
CXorf21	0.94872	2.47E-24
NLRC5	0.7045897	2.51E-24
HMOX1	0.6982103	2.51E-24
C1S	1.00247	2.55E-24
FCRL6	1.3493059	2.57E-24
ADAR	0.3782815	2.65E-24
MS4A7	0.9714485	2.68E-24
PMP22	0.7897337	2.81E-24
CD69	1.1164576	3.18E-24
MPEG1	0.9840485	3.44E-24
TRAFD1	0.3071066	3.95E-24
APOC1	1.2288464	3.98E-24
AQP9	1.6272999	4.71E-24
JAK2	0.6773246	6.06E-24
HNRNPA1P21	0.8914519	6.35E-24
HLA.F	0.852632	6.66E-24
GPR65	0.8867442	6.81E-24
PML	0.5210771	7.94E-24
GNGT2	0.6971041	8.71E-24
CTSK	0.9396132	8.92E-24
BLVRA	0.7918929	9.78E-24

TRGC2	0.84442236	8.63E-11
FASLG	0.77806636	8.66E-11
TNFRSF18	0.58084116	9.09E-11
CCL3	0.7465966	9.12E-11
ZSCAN1	0.63044372	9.15E-11
EVI2B	0.61898802	9.45E-11
MICB	0.59134502	9.65E-11
NCF2	0.64506453	9.90E-11
DOCK10	0.48869572	1.03E-10
EVL	0.46743969	1.06E-10
CSF1R	0.64431779	1.07E-10
HLA.DQB2	0.90959913	1.24E-10
MS4A4A	0.69533355	1.27E-10
DDX60	0.53672653	1.30E-10
IGSF6	0.5382351	1.56E-10
SLC31A2	0.48708773	1.56E-10
ZBED2	0.97149659	1.58E-10
HLA.S	0.87464724	1.58E-10
DPEP2	0.56118464	1.61E-10
BTK	0.5697479	1.69E-10
EIF4E3	0.44496056	1.70E-10
GPR108	0.2385617	1.72E-10
C3AR1	0.64890663	1.74E-10
HIVEP3	0.43174414	1.80E-10
IL9R	0.74662166	1.84E-10
ITGAX	0.62246001	1.88E-10
AIF1	0.49349895	1.88E-10
HRH2	0.81430643	2.02E-10
ARSA	0.34765669	2.06E-10
KLHDC7B	0.67828894	2.07E-10
MPEG1	0.63228528	2.13E-10
PMP22	0.50364133	2.17E-10
GPR174	0.94922374	2.28E-10
TLR6	0.56670458	2.33E-10
NTRK1	0.71378342	2.39E-10
TCAF2	0.54292991	2.43E-10
JAKMIP1	0.70595351	2.45E-10
TMEM140	0.30565896	2.45E-10
ACP5	0.54393795	2.54E-10
PILRA	0.59751536	2.97E-10
HLA.U	0.97626112	3.17E-10
PRKCB	0.62219093	3.21E-10
POU2F2	0.48188179	3.31E-10
GPR68	0.52651711	3.44E-10
SOCS3	0.52585482	3.44E-10
PCDHGC5	0.8749466	3.69E-10
CHST11	0.52123639	3.95E-10
SLC2A5	1.0128042	9.94E-24
CD33	0.8303774	1.07E-23
NRP1	0.8206727	1.11E-23
CSF1R	0.9733759	1.20E-23
GGTA1P	0.8901596	1.23E-23
IL12RB1	0.8960118	1.42E-23
CD180	0.9381271	1.58E-23
TRBC2	0.9406545	1.63E-23
SCPEP1	0.6324906	1.79E-23
ALOX5AP	0.8496291	1.95E-23
GIMAP6	0.7606238	1.96E-23
GZMH	1.23112	2.11E-23
FLI1	0.6645723	2.15E-23
OAS1	0.6230532	2.20E-23
LAMP3	0.7450761	2.29E-23
PLSCR1	0.4742176	2.41E-23
THEMIS2	0.7174693	2.54E-23
NCF1C	1.0028766	2.64E-23
OPTN	0.4538448	2.72E-23
TOMM20P2	1.3078651	3.25E-23
JAKMIP1	1.0786908	3.33E-23
CCL13	1.7936367	3.42E-23
LILRA6	1.0311225	3.43E-23
IL10	1.137651	3.47E-23
HVCN1	0.5615503	3.56E-23
OLR1	1.4723777	3.68E-23
GZMA	1.1422061	3.79E-23
FOXP3	0.7814132	4.07E-23
ZNF804A	1.28496	4.14E-23
ARL4C	0.8915633	4.62E-23
ZEB2	0.8409857	4.74E-23
GPR174	1.4589102	4.94E-23
SIGLEC7	1.0221151	6.19E-23
MRC1	1.2488813	6.95E-23
TRBV28	0.8883284	7.21E-23
FAM26F	1.0882139	7.36E-23
TIMP2	0.9327366	7.49E-23
TRAV3	1.4035162	8.03E-23
LIPA	0.5592236	8.28E-23
LIMD2	0.6906875	9.74E-23
MSN	0.7134791	1.00E-22
PRKCB	0.9528067	1.05E-22
FGD2	0.7062435	1.07E-22
ADAP2	0.5607991	1.16E-22
ST8SIA4	0.7414708	1.19E-22
MAP4K1	0.7996243	1.25E-22
NRIR	1.4836873	1.31E-22

TRAT1	0.82601848	4.00E-10
TNFSF10	0.36816013	4.16E-10
PPP1R18	0.41682979	4.17E-10
CBY3	0.82898875	4.29E-10
TRBV18	0.8336601	4.45E-10
GNLY	0.81275632	4.46E-10
TNIP1	0.20168649	4.49E-10
MS4A6A	0.59554344	4.66E-10
LIMD2	0.44979522	4.69E-10
VMO1	0.54883222	4.94E-10
PPP1R16B	0.54205109	5.18E-10
ZAP70	0.60308952	5.21E-10
GYPC	0.47513564	5.23E-10
PML	0.33025402	5.25E-10
FCER1G	0.57963138	5.36E-10
SIRPB2	0.61346583	5.44E-10
BST2	0.78986715	5.55E-10
ACKR4	0.88686917	5.57E-10
IFITM4P	0.83298152	5.58E-10
KIR2DL4	1.02025561	5.92E-10
ITGB7	0.61761294	6.03E-10
IFI6	0.72723584	6.07E-10
CREB3	0.2384122	6.95E-10
LAT2	0.37862674	7.03E-10
TNFRSF8	0.53870942	7.06E-10
HLA.F.AS1	0.47953637	7.16E-10
B3GALT4	0.36921524	7.59E-10
TSPAN4	0.46301122	7.70E-10
SNAI3	0.5326978	7.73E-10
CD79B	0.6166064	7.89E-10
USF1	0.22287121	8.46E-10
PDCD1LG2	0.71138195	8.96E-10
OAS2	0.70628778	9.03E-10
CD1D	0.44204759	9.13E-10
PLEKHO2	0.40010964	9.22E-10
ZNF804A	0.79675002	9.32E-10
FLI1	0.41804356	9.50E-10
SAMD9	0.5899858	9.52E-10
CLEC4G	0.92580938	9.95E-10
CD101	0.38853766	1.04E-09
TESPA1	0.57658437	1.05E-09
CYBB	0.63509357	1.06E-09
HVCN1	0.35374921	1.07E-09
RHOG	0.24420639	1.07E-09
LMF2	0.29283244	1.08E-09
NFATC1	0.54398762	1.09E-09
CARD16	0.43416319	1.10E-09
FASLG	1.1505012	1.31E-22
GAB3	0.5942056	1.32E-22
CCR2	1.1884154	1.53E-22
RCSD1	0.6831064	1.55E-22
CD247	0.7960617	1.60E-22
CCR8	1.1884063	1.68E-22
TRBV19	1.310203	1.70E-22
SIRPG	0.9905649	1.72E-22
TTC24	1.4625452	1.87E-22
ENTPD1	0.4744904	1.87E-22
CPVL	0.9802772	1.92E-22
GPR171	1.1297639	1.93E-22
PDE6G	0.9076082	1.93E-22
MRAS	0.8299263	2.24E-22
CCDC88A	0.8299384	2.33E-22
BATF2	0.7579468	2.35E-22
STAT4	0.7011715	2.41E-22
TM6SF1	0.9371607	2.68E-22
CARD17	1.4537274	2.96E-22
GPR141	1.3388382	3.32E-22
WIPF1	0.7073703	3.41E-22
NFAM1	0.7048778	3.53E-22
RNF213	0.6039043	3.70E-22
RASSF2	0.7581478	3.74E-22
DRAM1	0.5590374	3.92E-22
SERPINF1	0.8577416	4.21E-22
BASP1	0.845902	4.72E-22
C1R	0.8637189	4.74E-22
TNFAIP6	1.2406208	4.83E-22
TMEM140	0.4547261	5.12E-22
DPEP2	0.8228936	5.70E-22
CTHRC1	1.1440379	6.09E-22
CYSLTR2	1.0793701	6.82E-22
ABI3	0.6161554	7.12E-22
GIMAP1	0.6190052	7.64E-22
FTH1P22	1.2898387	7.77E-22
DSE	0.7669848	7.77E-22
TESPA1	0.8838026	8.50E-22
LUM	1.1165104	8.54E-22
AXL	0.7605338	9.91E-22
DTHD1	1.4720414	1.08E-21
SLC37A2	1.0354123	1.10E-21
EIF2AK2	0.4081034	1.13E-21
HLA.B	0.6774056	1.24E-21
KCNK13	0.8879657	1.24E-21
NR3C1	0.7477492	1.34E-21
SNX10	0.7375203	1.36E-21

FERMT3	0.51009539	1.14E-09
CECR1	0.62269407	1.17E-09
FBLN7	0.44260842	1.25E-09
CNR2	0.87810542	1.26E-09
CXCL16	0.34839074	1.28E-09
CRTAM	0.87918827	1.31E-09
ISG15	0.60903542	1.32E-09
LILRB5	0.67476425	1.35E-09
IFIH1	0.3750656	1.42E-09
FCRL3	0.90231646	1.53E-09
STX4	0.21480005	1.55E-09
DERL3	0.62765527	1.56E-09
FYB	0.59443367	1.57E-09
CITED2	0.30355649	1.57E-09
PLA2G2D	1.13432353	1.61E-09
CD209	0.69666822	1.61E-09
STAB1	0.51404713	1.62E-09
CCL19	1.04634425	1.63E-09
CD69	0.68053413	1.63E-09
TRAV17	0.81630284	1.68E-09
SPN	0.51143813	1.75E-09
CLECL1	0.77783248	1.82E-09
CXCR4	0.56766886	1.87E-09
PIP4K2A	0.2513827	1.94E-09
C10orf10	0.56159675	1.99E-09
CYP4F22	0.74346883	2.00E-09
SCARF1	0.34637673	2.01E-09
C2	0.51781585	2.05E-09
FCRL1	1.05178168	2.07E-09
GPR171	0.7122134	2.07E-09
FCGR2A	0.56363659	2.17E-09
SAMHD1	0.36409445	2.24E-09
FCGR3A	0.7700248	2.27E-09
FOXP3	0.4863162	2.27E-09
MIR22HG	0.39272792	2.32E-09
CD163	0.78614868	2.37E-09
FAM20A	0.55229506	2.37E-09
SERPING1	0.60507258	2.42E-09
SAMSN1	0.55035721	2.49E-09
PYHIN1	0.68271936	2.59E-09
CR1	0.86294805	2.68E-09
MICE	0.64690791	2.70E-09
LCP1	0.59270531	2.75E-09
TRAV2	0.82671029	2.76E-09
P2RY10	0.75740502	2.78E-09
NLRP1	0.47336975	2.84E-09
MARK2P9	0.76666944	2.88E-09
TRGC2	1.2267605	1.40E-21
DNAJC5B	1.1624171	1.68E-21
CLEC12A	1.3004808	1.83E-21
OSCAR	0.8414066	1.89E-21
CR1	1.348205	2.00E-21
ZNF683	1.5222471	2.13E-21
MYO5A	0.715103	2.19E-21
MEFV	1.1568446	2.23E-21
HLA.DOB	0.9542632	2.60E-21
DCSTAMP	1.5680492	2.66E-21
NFATC1	0.8323894	2.75E-21
ETV7	0.8062382	3.10E-21
CLMP	0.9192358	3.14E-21
POSTN	1.3256821	3.15E-21
STOM	0.6986391	3.20E-21
TNFSF10	0.5454267	3.50E-21
SLFN11	0.8161261	3.66E-21
C3	1.318632	3.79E-21
CLEC4D	1.468656	3.83E-21
TLR6	0.8287632	3.86E-21
GBP6	1.3498717	4.38E-21
TNFSF14	0.867224	4.69E-21
AD000864.6	0.8713274	5.68E-21
CTSW	1.1620741	6.93E-21
XCL2	1.360049	7.29E-21
SPHK1	0.9739985	7.36E-21
CTLA4	0.8674134	7.93E-21
TRGC1	1.2363406	8.09E-21
PLA2G2D	1.721291	8.25E-21
ALPK2	0.9598717	8.51E-21
NNMT	0.8946907	8.67E-21
HTRA4	1.1407171	8.87E-21
SIRPB1	1.2173692	9.72E-21
P2RY10	1.1635726	1.03E-20
SLAMF1	0.8175494	1.09E-20
TLR2	0.7747297	1.20E-20
FAM129A	0.8632718	1.34E-20
ODF3B	0.7810197	1.34E-20
RAB42	0.7188761	1.50E-20
CASS4	0.8199316	1.52E-20
PRF1	1.0037368	1.83E-20
TBC1D10C	0.8013904	1.86E-20
CD28	0.8229312	1.91E-20
APOL4	0.883459	1.96E-20
CD3D	0.8866955	2.04E-20
IL1RN	1.1103261	2.11E-20
RGS1	0.9709329	2.15E-20

JAK2	0.40700009	2.97E-09	*EMP3*	0.6836751	2.28E-20
IFIT5	0.35770219	3.03E-09	*KIR2DL4*	1.4841384	2.31E-20
FGL2	0.6048821	3.14E-09	*TNFRSF8*	0.7895021	2.31E-20
ARRDC5	0.72999016	3.25E-09	*VSIG4*	1.1407544	2.47E-20
CD244	0.67815282	3.28E-09	*SERPINB9*	0.5109411	2.51E-20
LINC00519	0.7636086	3.31E-09	*SH2B3*	0.4838674	2.57E-20
CSF3R	0.71071333	3.34E-09	*DCN*	1.0789203	2.64E-20
NCR1	0.87294915	3.59E-09	*SUCNR1*	1.1753339	2.65E-20
GRN	0.27927669	3.64E-09	*RTP4*	0.7434405	2.72E-20
FCGR2B	0.70260651	3.76E-09	*CD7*	0.992833	2.77E-20
MEI1	0.52940919	4.15E-09	*TRGV10*	1.3889731	2.83E-20
APOE	0.83355831	4.16E-09	*KYNU*	0.9094754	2.84E-20
STAT2	0.30425681	4.18E-09	*VAMP5*	0.7007205	2.86E-20
TRAV3	0.84529727	4.25E-09	*LAT2*	0.5557773	2.98E-20
TRIM38	0.23592405	4.27E-09	*SDS*	0.8641041	3.54E-20
TNFRSF9	0.53603879	4.44E-09	*TRANK1*	0.5822161	3.80E-20
P2RY8	0.4554441	4.45E-09	*CD40*	0.8251795	4.06E-20
LYL1	0.35851802	4.46E-09	*IKZF3*	0.9465938	4.13E-20
MX1	0.63395029	4.51E-09	*DHX58*	0.522092	4.25E-20
CCL18	1.11320944	4.69E-09	*MITF*	0.8193566	4.77E-20
CCR1	0.52368498	4.80E-09	*SULF1*	1.1638371	5.04E-20
CYSLTR2	0.67266405	4.81E-09	*SELPLG*	0.7381559	5.09E-20
ADAP2	0.34172698	5.06E-09	*LY9*	1.0216736	5.16E-20
HLA.V	1.01792495	5.07E-09	*RASGRP1*	0.8131915	5.27E-20
DAPK1	0.64856133	5.10E-09	*CXCR6*	0.8681274	5.61E-20
ARFGAP3	0.29041282	5.11E-09	*WDFY4*	0.8778255	5.61E-20
TNFRSF4	0.44225429	5.23E-09	*FRMD6*	0.8543936	5.63E-20
CXCL11	0.95459777	5.27E-09	*HRH2*	1.1412333	5.76E-20
APOBEC3H	0.60140984	5.44E-09	*SFMBT2*	0.7251141	5.91E-20
GIMAP4	0.43863899	5.56E-09	*FCRL3*	1.3391793	6.34E-20
DNAJC5B	0.72793333	5.80E-09	*JAK3*	0.6074639	6.64E-20
FOLR2	0.69952845	5.90E-09	*AVPR1A*	1.0563725	6.82E-20
C3	0.82711988	5.93E-09	*CCDC80*	1.1688597	7.15E-20
CST7	0.58898177	6.28E-09	*C19orf38*	0.826148	7.55E-20